https://doi.org/10.5194/egusphere-2026-2799
Preprint. Discussion started: 1 June 2026

Estimates of carbonyl sulfide and methane stratospheric lifetimes based on AirCore profiles

Alessandro Zanchetta[1], Steven van Heuven[1], Rigel Kivi[3], Michel Ramonet[4], Andreas Engel[5], Maarten Krol[6,7], and Huilin Chen[1,2]

[1] Center for Isotope Research (CIO), Energy and Sustainability Research Institute Groningen (ESRIG), University of Groningen, Groningen, the Netherlands
[2] Joint International Research Laboratory of Atmospheric and Earth System Sciences, School of Atmospheric Sciences, Nanjing University, Nanjing, China
[3] Space and Earth Observation Centre, Finnish Meteorological Institute (FMI), Sodankylä, Finland
[4] Laboratoire des Sciences du Climat et l'Environnement (LSCE), CEA - CNRS - UVSQ - University Paris-Saclay, Gif sur Yvette, France
[5] Institute for Atmospheric and Environmental Sciences, University of Frankfurt, Frankfurt, Germany
[6] Meteorology and Air Quality, Wageningen University & Research, Wageningen, the Netherlands
[7] Institute for Marine and Atmospheric Research, Utrecht University, Utrecht, the Netherlands

Correspondence to: Huilin Chen (huilin.chen@nju.edu.cn, huilin.chen@rug.nl)

Abstract

Stratospheric loss is a major sink for both carbonyl sulfide (COS) and methane (CH_4), but their stratospheric lifetimes and sinks remain poorly constrained because high-resolution observations of their vertical distributions in the lower stratosphere are sparse. Here, we estimate the mean stratospheric lifetime and sink of COS and CH_4 from their correlations with N_2O using two distinct methods applied to AirCore vertical profile measurements from three Northern Hemisphere summer campaigns. From these profiles, we derive a COS stratospheric lifetime of 69–90 years, corresponding to a sink of 30–41 GgS yr^{-1}. For CH_4, we find a stratospheric lifetime of 149–168 years, corresponding to a sink of 23–26 TgC yr^{-1}. These values are in good agreement with previous estimates (39–76 years for COS, 152-160 years for CH_4) and with estimates based on ACE-FTS observations (75–76 years for COS, 146–172 years for CH_4). As has been noted previously, we also find a decline in the COS tropospheric burden between 2016 and 2020 in our AirCore samples, in contrast to the continued growth of CH_4 and N_2O. In addition, we found that tracer-tracer correlations vary among flights, and even within the same campaign, pointing to variability in lower-stratospheric composition. Although this variability may reflect differences in stratospheric transport, its origin remains unclear and requires further investigation. These results provide observational constraints on the stratospheric budgets of COS and CH_4 and help refine their representation in atmospheric chemistry and transport models.

https://doi.org/10.5194/egusphere-2026-2799
Preprint. Discussion started: 1 June 2026

1. Introduction

Carbonyl sulfide (COS or OCS) is the most abundant sulfur-containing gas species in the atmosphere, with a tropospheric mole fraction of 350–550 ppt (Remaud et al., 2023; Whelan et al., 2018). Following evidence of COS uptake in plants at leaf level, this species has been suggested as a proxy to separate gross primary productivity (GPP) from respiration in plants, to deepen the understanding of carbon exchange between atmosphere and vegetation (Stimler et al., 2010, 2012; Whelan et al., 2018). Some recent studies, however, observed bidirectional COS exchange in some species under drought conditions, which may complicate the application of this tracer as a GPP proxy (Cho et al., 2025; Spielmann et al., 2025). Moreover, recent studies evidenced a mismatch between models and observations, pointing towards unidentified or poorly quantified processes that may also contribute to COS uptake, which may also undermine its usefulness as a GPP proxy (Kaushik et al., 2026).

COS has a relatively long lifetime in the troposphere (2–2.5 years) and is therefore able to enter the stratosphere (Ma et al., 2021; Montzka et al., 2007; Remaud et al., 2023). In the stratosphere, it is converted to precursors of sulfuric acid (which is converted to sulfate stratospheric aerosols) by photolysis and by reactions with OH• and O• radicals (Brühl et al., 2012; Chin and Davis, 1995; Krysztofiak et al., 2015). However, the assessments of both the mass budget and the contribution of COS to the formation of the stratospheric aerosol layer have not found full agreement yet (Krysztofiak et al., 2015; Vernier et al., 2011; Wilson et al., 2008). So far, the efforts to measure stratospheric COS have been based on remote sensing techniques (Bernath, 2005; Boone et al., 2023; Glatthor et al., 2017; Hannigan et al., 2022; Leung et al., 2002; Toon, 1991; Velazco et al., 2011), whole air samples (Engel and Schmidt, 1994) or in-situ spectrometry (Gurganus et al., 2025; Kloss et al., 2019; Krysztofiak et al., 2015).

Atmospheric lifetimes are useful quantities to assess the environmental impact of a gas species when emitted into the atmosphere (Volk et al., 1997). Typically, lifetimes are defined as the ratio between the global total atmospheric burden of a species and its sinks. When estimating partial lifetimes with respect to stratospheric loss, the ratio is defined focusing only on stratospheric sink. For species with only stratospheric sinks, atmospheric and stratospheric lifetimes are equal (Brown et al., 2013; Volk et al., 1997). In this study, we present estimates of COS average stratospheric lifetime and sink from observations performed at mid- and polar latitudes, inferred from their stratospheric correlation with nitrous oxide (N_2O) (Barkley et al., 2008; Engel and Schmidt, 1994; Karu et al., 2023; Krysztofiak et al., 2015; Plumb and Ko, 1992), obtained as continuous vertical profiles with AirCore samplers (Karion et al., 2010; Zanchetta et al., 2026) combined with a Quantum Cascade Laser Spectrometer (QCLS, Aerodyne Research Inc., MA, USA, model TILDAS-CS). This technique allows the collection of continuous atmospheric profiles and their analysis with minimal preparation and treatment, reducing contamination risks during field campaigns. The analysis on the QCLS allows for the simultaneous measurement of COS, N_2O, CH_4, CO_2 and CO. AirCore samplers were deployed in three different campaigns, namely Trainou (TRN, 47°58' N, 2°06' E), Kiruna (KRN, 67°53' N, 21°04' E) and Sodankylä (SOD, 67°22’ N, 26°37’ E). The results will be compared with ACE-FTS (Bernath, 2005; Boone et al., 2023; Velazco et al., 2011) spatially and temporally averaged observations, as well as with estimates from previous studies. We also present estimates of methane (CH_4) lifetime and sink following the same methodology.

https://doi.org/10.5194/egusphere-2026-2799
Preprint. Discussion started: 1 June 2026

2. Methodology

As thoroughly described in Zanchetta et al. (2026) and summarized in Table 1, AirCore samples were collected during three distinct balloon campaigns. The first campaign took place at mid-latitudes in Trainou (TRN, France), while the latter two were realized at polar latitudes in Kiruna (KRN, Sweden) and Sodankylä (SOD, Finland). Sampling, measurements and data processing will be briefly presented in the coming sections.

Table 1: locations and dates of the performed sampling campaigns. The flight codes correspond to the ones presented in (Zanchetta et al., 2026).

Location and coordinates	Date	Flight code	Instrument features	Inlet features
Trainou, France (TRN) 48°57' N, 2°06' E	17/06/2019	TRN1	23 m x Ø 8 mm + 46 m x Ø 4 mm V ~ 1600 cm^3	Free inlet
	18/06/2019	TRN2	36 m x Ø 3/16" + 38 m x Ø 1/8" V ~ 830 cm^3	$Mg(ClO_4)_2$ dryer
	18/06/2019	TRN3	23 m x Ø 8 mm + 46 m x Ø 4 mm V ~ 1600 cm^3	Free inlet
	20/06/2019	TRN4	36 m x Ø 3/16" + 38 m x Ø 1/8" V ~ 830 cm^3	Free inlet
Kiruna, Sweden (KRN) 67°53' N, 21°04' E	13/08/2021	KRN-a	37 m x Ø 3/16" + 39 m x Ø 1/8" V ~ 860cm^3	$Mg(ClO_4)_2$ dryer
	13/08/2021	KRN-b	36 m x Ø 3/16" + 38 m x Ø 1/8" V ~ 830 cm^3	Free inlet
Sodankylä (SOD) 67°25' N, 26°35' E	02/08/2023	SOD1	40 m x Ø 1/4" + 58 m x Ø 1/8" V ~ 1400 cm^3 Differential pressure sensors	$Mg(ClO_4)_2$ dryer
	05/08/2023	SOD3-a SOD3-b	200 m x Ø 1.5 mm" V ~ 1400 cm^3 Double-sided sampling	One side free inlet (a), one side cotton-based O_3 scrubber (b)
	08/08/2023	SOD5	40 m x Ø 1/4" + 58 m x Ø 1/8" V ~ 1400 cm^3 Differential pressure sensors	$Mg(ClO_4)_2$ dryer and cotton-based O_3 scrubber

2.1 AirCore sampling

An AirCore sampler (Karion et al., 2010) consists of a coil made of stainless-steel tube, internally coated with Sulfinert® (SilcoNert® 2000) to minimize destructive interactions between steel and gas species. When deployed on stratospheric

https://doi.org/10.5194/egusphere-2026-2799
Preprint. Discussion started: 1 June 2026

sounding balloons, it allows the passive collection of continuous vertical samples during the descent phase, thanks to the atmospheric pressure gradient (Karion et al., 2010; Membrive et al., 2017; Wagenhäuser et al., 2021). The sample is analyzed immediately after the flight on a continuous flow gas analyzer. Assuming pressure equilibrium, the pressure and temperature radiosonde readings can be used to calculate the sampled amount of air (in moles) for any time interval. Knowing the analyzed number of moles it is possible to link each aliquot to the sampling altitude and, therefore, retrieve the collected altitude profile (Karion et al., 2010; Membrive et al., 2017; Tans, 2022). The profiles of this study were retrieved following the approach described in Membrive et al. (2017), except for the one collected with University of Bern's double-sided AirCore. One half of this AirCore was equipped with an O_2 injection system. The injections were programmed at specific altitudes (namely, at 21045.2, 17005.2, 11837.0, 7869.9 and 4592.2 m) to help the altitude retrieval process, similarly to the method described for CO in Wagenhäuser et al. (2021). These injections caused contamination spikes in the COS profile and were therefore visible in our analysis, which allowed the altitude retrieval process.

2.2 Quantum Cascade Laser Spectrometer (QCLS)

All AirCore samples have been analyzed on a dual laser QCLS (Aerodyne Research Inc., Billerica, MA, USA), an absorption spectrometer covering the mid-infrared (IR) frequencies range. Analysis of COS with mid-IR spectrometry was first described by Stimler et al. (2009). The instrument deployed in this study has been previously introduced in Vinković et al. (2022) and Tong et al. (2023). The QCLS measures CH_4, CO_2, N_2O, CO, COS and O_3 simultaneously and features a custom-made frontend, designed specifically for AirCore use. The operating parameters and the achieved measurement precision for each gas species are reported in Table 2.

Table 2: QCLS operating parameters and achieved precisions.

Parameter	Value
Temperature	~ 298 ± 0.002 K
Pressure	~ 50 ± 0.005 Torr (66 hPa)
Sample mass flow	~ 50 mL min^{-1}
Measurements frequency	1 Hz
Geometric cell volume	150 cm^3
Effective cell volume	~10 cm^3
N_2O measurement precision	0.12 ppb
CH_4 measurement precision	0.6 ppb
CO_2 measurement precision	0.2 ppm
CO measurement precision	1 ppb
COS measurement precision	20 ppt
H_2O measurement precision	20 ppm

https://doi.org/10.5194/egusphere-2026-2799
Preprint. Discussion started: 1 June 2026

O_3 measurement precision	0.1 ppm

2.3 ACE-FTS observations

Similarly to Zanchetta et al. (2026), ACE-FTS observations were used as a validation tool of AirCore results. Conceptually, obtaining consistent results from two very different observational methodologies should provide proof of the reliability of both techniques. ACE-FTS is a satellite-borne spectrometer retrieving the altitude profiles of temperature, pressure and mole fractions of several gas species between 0–150 km altitude with a resolution of 1 km (Bernath, 2005; Glatthor et al., 2017; Velazco et al., 2011). The spectrometer retrieves profiles using solar occultation during sunset and sunrise. This limits the amount of measurable profiles, but enhances their vertical resolution (Bernath, 2005). Among its observations, ACE-FTS includes COS, N_2O and CH_4, which allows the calculation of stratospheric lifetimes (Sect. 2.4). ACE-FTS v5.3 data (Boone et al., 2023) have been filtered to obtain a dataset complementary to the measured AirCore profiles. To stay close to the conditions of the campaigns, ACE-FTS observations of COS, N_2O and CH_4 in summer months (June–September) after 2012 were selected between 45°-49° N for Trainou and between 65°-69° N for Kiruna and Sodankylä, respectively. The resulting 502 mid-latitude and 1681 polar latitude ACE-FTS profiles were averaged for each latitudinal interval. The resulting two averaged profiles were then treated identically to the AirCore-derived profiles (as described in Sect. 2.4) to calculate COS and CH_4 stratospheric lifetimes, and these mostly independent lifetime estimates are compared in Sect. 3.

2.4 Calculation of stratospheric lifetimes according to Plumb and Ko (1992)

Plumb and Ko (1992) described a method to calculate the stratospheric lifetime of a tracer. While for species with purely stratospheric sink the stratospheric lifetimes derived in this way are equal to the global lifetimes, they are only partial lifetimes for species with additional sinks in the atmosphere. The method further requires species to be in steady state and show an identifiable linear correlation in the lower stratosphere. If these conditions are met and the stratospheric lifetime of one species is known, then it is possible to calculate the stratospheric lifetime of another tracer, following:

$$\frac{T_1}{T_2} \cong \frac{d\sigma_2}{d\sigma_1} * \frac{\sigma_1}{\sigma_2} \qquad (1)$$

Where T_x is the stratospheric lifetime of a species, σ_x a mole fraction representative of the tracer's atmospheric abundance, and $d\sigma_2/d\sigma_1$ is the slope of the tracer-tracer correlation in the lower stratosphere. For simplicity, we assume that the ratio of the atmospheric mean mole fractions can be approximated by the ratio of representative tropospheric mean mole fractions.

This method has been used to estimate the stratospheric lifetime of COS in various studies (Barkley et al., 2008; Engel and Schmidt, 1994; Karu et al., 2023; Krysztofiak et al., 2015). Specifically, Barkley et al. (2008) and Engel and Schmidt (1994) calculated the COS lifetime using its correlation with CFC-12, while Karu et al. (2023) and Krysztofiak et al. (2015) used its correlation with N_2O. In this study, we will estimate the lifetimes of COS and CH_4 using their stratospheric correlations with N_2O. Rearranging Eq. 1, we obtain:

https://doi.org/10.5194/egusphere-2026-2799
Preprint. Discussion started: 1 June 2026

$$T_x \cong \frac{d\sigma_{N_2O}}{d\sigma_x} * \frac{\sigma_x}{\sigma_{N_2O}} * T_{N_2O}, with\ x = COS, CH_4 \quad (2)$$

Each variable at the right-hand side of the equation has an uncertainty. These uncertainties were propagated into an overall uncertainty of the lifetime estimate. The methods used to estimate T_{N_2O}, σ_{x,N_2O} and $d\sigma_{N_2O}/d\sigma_x$ and their associated uncertainties will be described in Sect. 2.4.1, 2.4.2, and 2.4.3, respectively.

2.4.1 N_2O lifetime

The N_2O stratospheric lifetime is relatively well-known and has been estimated from reaction rates derived from vertical profiles of O_3 and temperature (Prather et al., 2015). Krysztofiak et al. (2015) adopted a lifetime of 117 ± 20 years (NOAA, 2003). Karu et al. (2023) used a T_{N_2O} of 116 ± 9 years, following the estimate of Prather et al. (2015). However, the N_2O lifetime has been reported to decrease consistently at a rate of -2.1 ± 1.2 % per decade between 2005 and 2021 (Prather et al., 2023). Moreover, the N_2O lifetime has been reported to depend on solar activity, which causes a variability of approximately 7 % (Prather et al., 2015). Therefore, to account for potential variations or unaccounted trends during our campaign period, we chose to infer N_2O lifetime in 2019, 2021 and 2023 starting from the 116 ± 9 years estimate (Prather et al., 2015), given the small –2.1 ± 1.2 % per decade decreasing trend (Prather et al., 2023) is not significant in such a short time span.

2.4.2 Tropospheric burdens

Previous studies estimating COS lifetime using the Plumb and Ko (1992) method used different approaches to define σ_{COS}. According to Plumb and Ko (1992), σ_x should be a representative tropospheric mole fraction value of the considered tracer. It is good to mention that the stratospheric lifetime of a tracer should result from the ratio of its global atmospheric burden and its stratospheric sink. However, since the species considered in this study are all long-lived and show similar features in terms of transport and kinetics, the ratio of their tropospheric burdens can be considered a rather good approximation of the ratio of their total atmospheric burdens. Previous studies adopted different estimates to represent the tracers' burdens. Engel and Schmidt (1994) arbitrarily adopted an average tropospheric value of 500 ppt. Similarly, Barkley et al. (2008) assumed a value of 500 ppt ± 20%. Krysztofiak et al. (2015) estimated an average tropospheric mole fraction of 550 ± 40 ppt from their in-situ observations. In contrast to Plumb and Ko's (1992), Karu et al. (2023) calculated σ_{COS} as 415 ± 32 ppt by averaging their stratospheric COS mole fraction observations. In this study, to obtain representative tropospheric mole fractions for COS, N_2O and CH_4, we followed the approach described in Andrews et al. (2001), which was previously used in other studies on age of air estimations (Andrews et al., 1999; Boering et al., 1996). Andrews et al. (2001) defined the stratospheric boundary conditions of CO_2 by averaging 12-months running means from surface data collected in Mauna Loa (19 °N, MLO) and American Samoa (14 °S, SMO), delayed by two months. Similarly, we calculated these means for each campaign for COS, N_2O and CH_4 and we estimated each species' tropospheric burden consequently using NOAA's data (Montzka et al., 2007, updated). The calculated average tropospheric mole fractions are presented in Figure 1 (the plots show 12-months running means and their standard deviations only every 6 months, for clarity). While the increase of N_2O and CH_4 is evident over time, it is interesting

https://doi.org/10.5194/egusphere-2026-2799
Preprint. Discussion started: 1 June 2026

to notice that COS mole fraction decreased between 2016 and 2020 and showed a general increase between 2020 and 2025 (Hannigan et al., 2022; Serio et al., 2023).

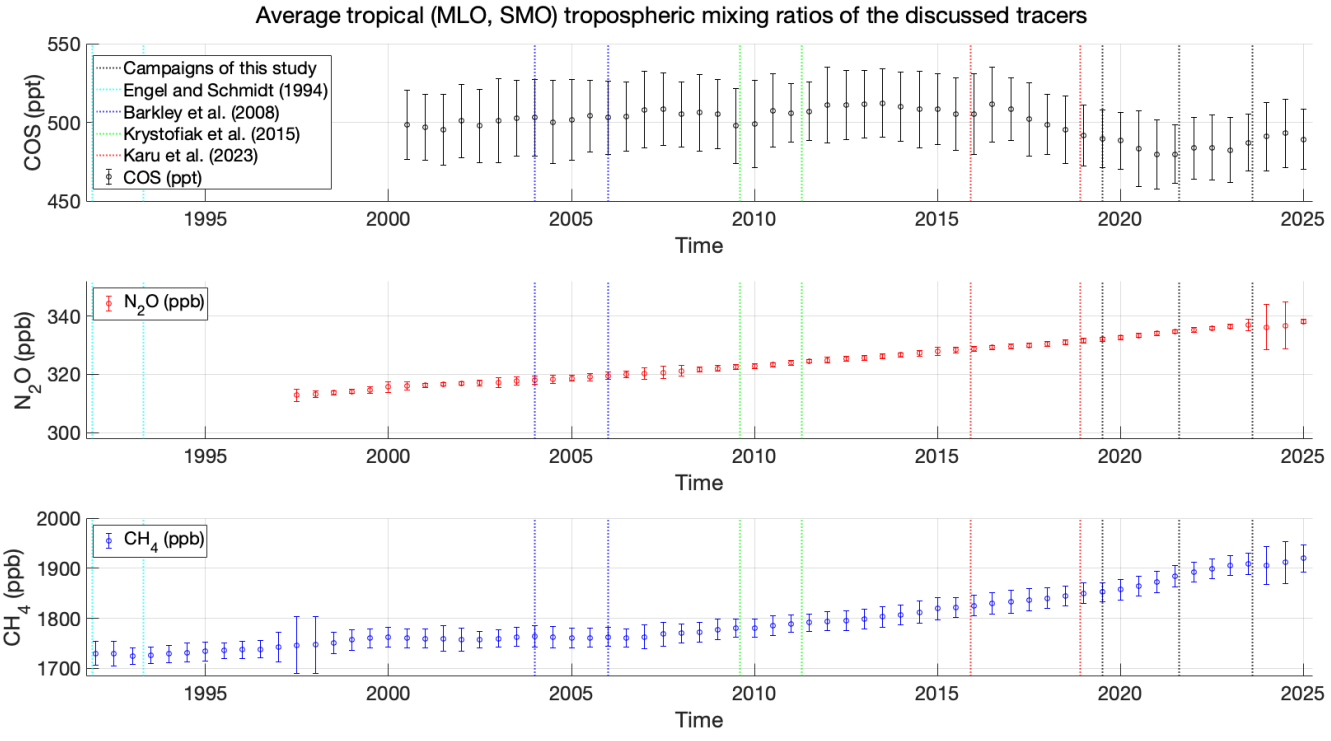

Figure 1: averaged MLO and SMO tropospheric mole fractions retrieved from NOAA's flask observations, from which the burdens were derived. The vertical lines represent flight dates of different campaigns. For Barkley et al. (2008) and Karu et al. (2023), they represent the start and end of the periods covered by their campaigns. The larger deviations observed for CH_4 around 1998 and for both N_2O and CH_4 around 2024 are due to unusually low mole fractions observed in SMO and do not affect the results of this study.

2.4.3 Data selection for calculating the slope from tracer-tracer correlations

The stratospheric part of the profiles (Figure 2a and Figure 3a) was defined using the definition of thermal tropopause (World Meteorological Organization (WMO), 1957), calculating the lapse rate from the radiosonde data collected during each flight (Zanchetta et al., 2026). However, as exemplified in Figure 2b and Figure 3b, a non-linear relationship between COS/CH_4 and N_2O was noticeable just above the thermal tropopause for all flights. Specifically, this deviation was observed in 2019 for N_2O mole fractions between 315 and 295 ppb, in 2021 between 310 and 325 ppb and in 2023 between 335 and 315 ppb. Likely, this is caused by a mixing of northern hemispheric tropospheric air with associated seasonality in both COS and CH_4 with stratospheric air in the lowermost stratosphere. Therefore, the linear correlation was determined for N_2O mole fractions lower than 295 ppb in TRN, to 298 ppb in KRN and to 300 ppb SOD, progressively increasing the threshold to reflect the tropospheric increase of N_2O. Similar features, although smoothed, were also present in the averaged ACE-FTS correlations, which were therefore limited to N_2O mole fractions lower than 300 ppb. Plumb and Ko (1992) stressed the importance of limiting the tracer-tracer correlation analysis to mole fraction intervals where a linearity between both tracers is present. N_2O is a tracer of

https://doi.org/10.5194/egusphere-2026-2799
Preprint. Discussion started: 1 June 2026

tropospheric origin with a stratospheric sink weak enough to make it long-lived throughout the lower stratosphere. If this condition is not fulfilled for another tracer, e.g. due to different stratospheric sinks (or sources) confined to specific stratospheric regions, the relationship between the species bends into a curve (see Sect. 4 in Plumb and Ko, 1992). In the collected AirCore samples, although there is no pronounced curvature, different linear relationships with COS can be found for N_2O mole fractions above and below 200 ppb (Figure 2c), or above and below N_2O mole fractions of 230 ppb for CH_4 (Figure 3c). These curvatures in the tracer-tracer relationships reflect different stratospheric chemistry over altitude affecting sources and/or sinks differently for each gas species (Plumb and Ko, 1992). Therefore, we limited the tracer-tracer correlations to the regions where a single-slope linearity between the species is respected, which corresponds to altitudes up to roughly 20 to 22 km. The two profiles obtained from SOD3 are cut at $N_2O \approx 280$ ppb due to contamination effects (see Zanchetta et al., 2026). The details of the resulting selections are listed in Table 3 and the selection processes are illustrated in Sect. S1 (COS) and Sect. S2 (CH_4) in the Supplement for all flights except for TRN2 (in Figure 2 and Figure 3).

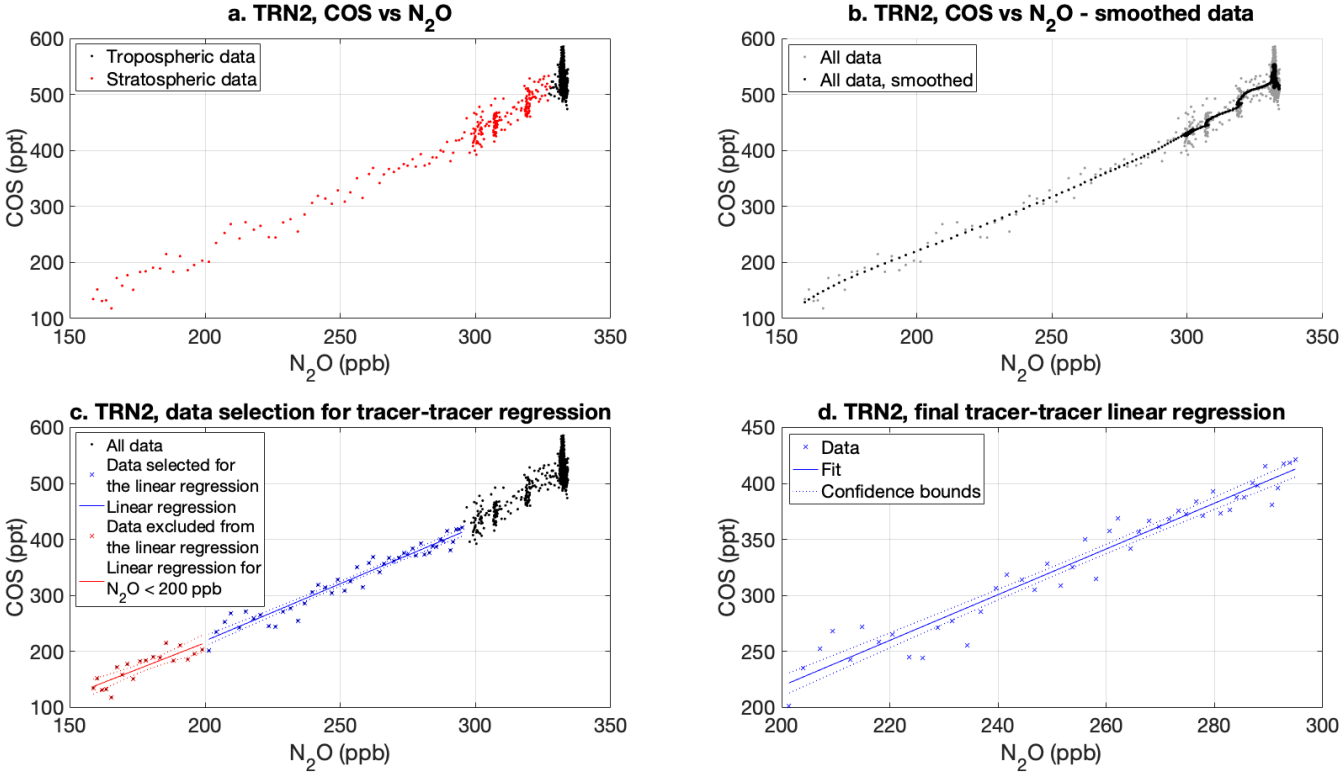

Figure 2: data selection steps for the linear regression between COS and N_2O, exemplified with the TRN2 AirCore data.

https://doi.org/10.5194/egusphere-2026-2799
Preprint. Discussion started: 1 June 2026

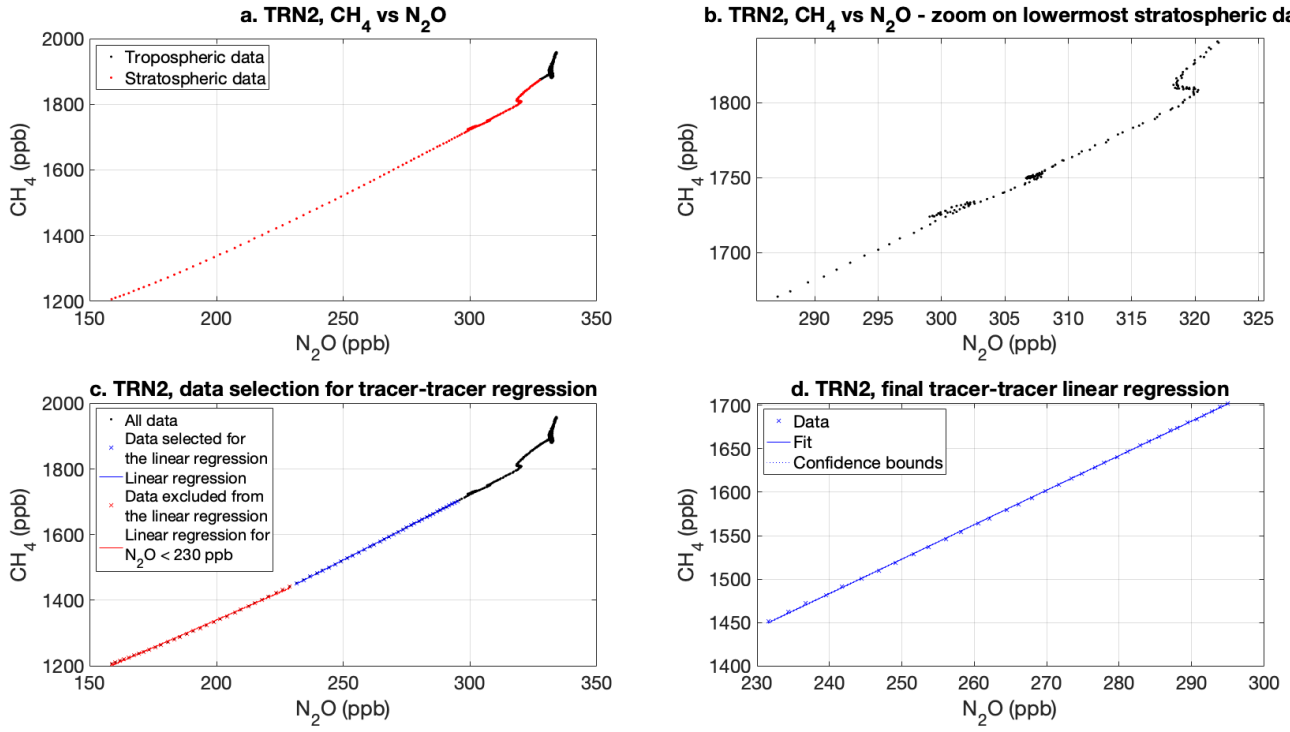

Figure 3: data selection steps for the linear regression between CH_4 and N_2O, exemplified with the TRN2 AirCore data.

Table 3: summary of refined data used for the tracer-tracer regressions after the selection procedure explained in Sect. 2.4.3. For TRN1 (*) no temperature nor humidity data was available and the tropopause was assigned arbitrarily at 11.0 km.

Date/period	Data origin	Thermal tropopause (km)	Altitude range of the selection for the COS-N_2O regression (km)	Data points for the COS-N_2O regression	Altitude range of the selection for the CH_4-N2O regression (km)	Data points for the CH_4-N_2O regression
17/06/2019	TRN1	11.0 *	17.3–20.9	77	17.3–20.0	62
18/06/2019	TRN2	11.5	18.3–22.2	47	18.3–21.0	36
18/06/2019	TRN3	10.8	17.9–21.5	64	17.9–20.4	48
20/06/2019	TRN4	10.6	17.3–20.6	43	17.3–19.4	31
13/08/2021	KRN-a	10.5	14.9–20.3	96	14.9–19.4	86
13/08/2021	KRN-b	10.5	14.9–20.3	93	14.9–19.4	82
02/08/2023	SOD1	10.9	16.1–20.7	116	16.1–20.0	102
05/08/2023	SOD3-a	9.2	16.8–18.4	22	16.8–18.4	22
05/08/2023	SOD3-b	9.2	16.5–16.5	1	16.5–16.5	1
08/08/2023	SOD5	10.6	16.8–20.9	66	16.8–20.2	53

https://doi.org/10.5194/egusphere-2026-2799
Preprint. Discussion started: 1 June 2026

June to September, 2012-2023	Polar (65°-69° N) average, ACE-FTS	/	15.5–20.5	6	15.5–18.5	4
June to September, 2012-2023	Mid-latitude (45°-49° N) average, ACE-FTS	/	17.5–21.5	5	17.5–20.5	4

2.4.4 Data deficiency and flagging of outliers

Due to the data selection described in Sect. 2.4.3, the tracer-tracer correlation dataset for flight SOD3-b was restricted to a single data point. Therefore, it was not possible to retrieve a correlation with the profiles measured after this flight.

Another AirCore flight (KRN-a) was marked as an outlier for COS. As shown in Table 4, the linear regression between N_2O and COS for KRN-a resulted in a much lower R-squared value and featured a much smaller slope than the other flights at polar latitudes did. Although in Zanchetta et al. (2026) the retrieved profile was comparable within uncertainties with previous stratospheric COS observations, between altitudes between roughly 17 and 20 km the profile was significantly lower than all other profiles (see Fig.2, 6 and 8 in Zanchetta et al., 2026). Since the data selected for the tracer-tracer correlation falls in the same range, this has probably biased the results of the regression. Overall, the reason for this discrepancy remained unclear, but we speculate it may have been due to issues during the COS measurements, caused either by instability of the QCLS analyzer, or by contamination during sampling or analysis.

2.5 Calculation of stratospheric lifetimes following Volk et al. (1997)

The method of Plumb and Ko (1992), described in the previous section and adopted in several previous studies (Barkley et al., 2008; Engel and Schmidt, 1994; Karu et al., 2023; Krysztofiak et al., 2015) assumes steady state for both tracers, implying a globally uniform stratospheric correlation between the two species and no significant long-term tropospheric trends. Volk et al. (1997) applied a more comprehensive formalism to this theory, refining its boundaries while still applying Eq. (2). To account for deviation from the “slope equilibrium” of Plumb and Ko (1992), Volk et al. (1997) advocates the extrapolation of the tracer-tracer slope at the (extratropical) tropopause, where the correlation shall be representative of the tracers’ vertical gradient. This would also prevent biases that may be observed (e.g., as curvatures in the tracer-tracer correlation slopes) due to non-diffusive mixing during transport from the tropics to mid latitudes. Moreover, this method requires global atmospheric burdens integrated over altitude, differently from the tropospheric burdens adopted by Plumb and Ko (1992). The assumptions on N_2O lifetime (Sect. 2.4.1) will be kept for this methodology. All other different steps adopted to apply this methodology are described in the following paragraphs.

https://doi.org/10.5194/egusphere-2026-2799
Preprint. Discussion started: 1 June 2026

2.5.1 Global atmospheric burdens

To obtain a representative estimate of global atmospheric burdens of COS, N_2O and CH_4, their mean tropospheric mole fraction was firstly inferred following the method of Andrews et al. (2001), similarly to what has been described in Sect. 2.4.2. The obtained averaged tropospheric mole fractions were assumed to be constant up to 10 km of altitude. Above this altitude, to estimate the average global stratospheric mole fractions, ACE-FTS data at tropical, mid and polar latitudes were averaged for each campaign's year (2019, 2021 and 2023). Likewise, the average global pressure profiles were retrieved from ACE-FTS data for each year. Both the tropospheric average and the averaged stratospheric mole fractions were then multiplied by the corresponding average pressure at each altitude, summed together and divided by the total pressure, obtaining a global average burden weighted by the contribution of each atmospheric layer over altitude. An example of the mole fraction profiles against pressure, used to estimate the global atmospheric burdens, is presented in Figure 4.

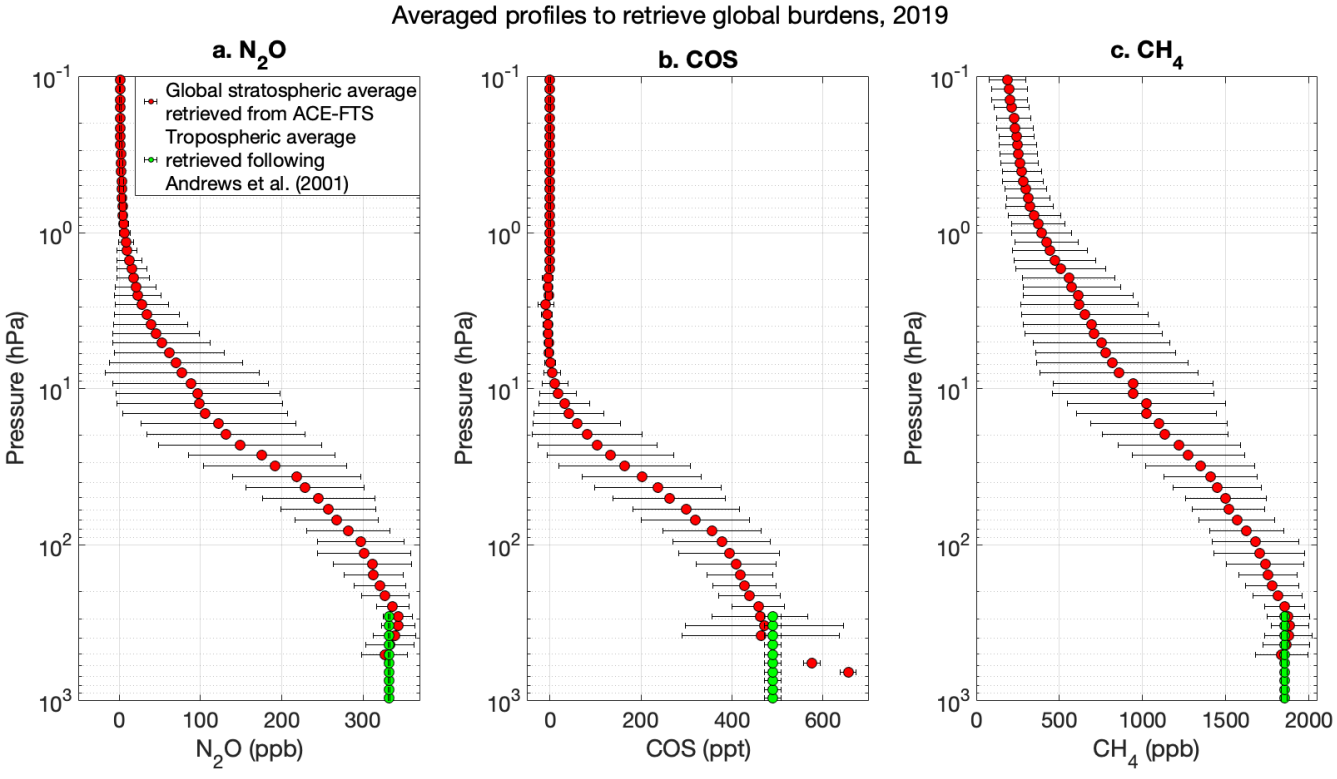

Figure 4: the average global profiles used to calculate the global average burdens for 2019. The red dots represent globally averaged ACE-FTS data, while the green dots are the tropospheric averages retrieved following Andrews et al. (2001). Where both data are present, only the averages retrieved with Andrews et al. (2001) method were considered.

2.5.2 Calculation of local stratospheric slopes and extrapolation of tracer-tracer slope at the tropopause

The method adopted to infer the local tracer-tracer slopes follows the approximations of previous studies (Brown et al., 2013; Laube et al., 2013; Leedham Elvidge et al., 2018; Volk et al., 1997). The correlation slopes between COS (or CH_4) and N_2O

https://doi.org/10.5194/egusphere-2026-2799
Preprint. Discussion started: 1 June 2026

were calculated every 3 ppb of N_2O, over N_2O ranges of 100 ppb. The N_2O range width was chosen to prevent biases due to, for example, annual cycles or other short-term processes that may cause deviations in the slope curvatures (Volk et al., 1997). The inferred local slopes against N_2O (used as a proxy for altitude mapping) are shown in Figure 5–7 for COS, and in Figure 8–10 for CH_4. The evident criticalities of TRN4, KRN-a and SOD3-b will be presented and discussed in Sect. 2.5.3. The lowermost slopes (N_2O > 300 ppb) were excluded from the slope analysis to prevent biases due to tropospheric air fluxes - which are not constant unless species are in steady state (Brown et al., 2013; Volk et al., 1997) - while the highest side of the profiles (N_2O < 200 ppb) were excluded due to non-uniform deviations from the expected curves (Volk et al., 1997). The uncertainties at the tropopause were inferred applying the bootstrap method (Laube et al., 2013; Leedham Elvidge et al., 2018; Volk et al., 1997) within the 200–300 ppb N_2O range.

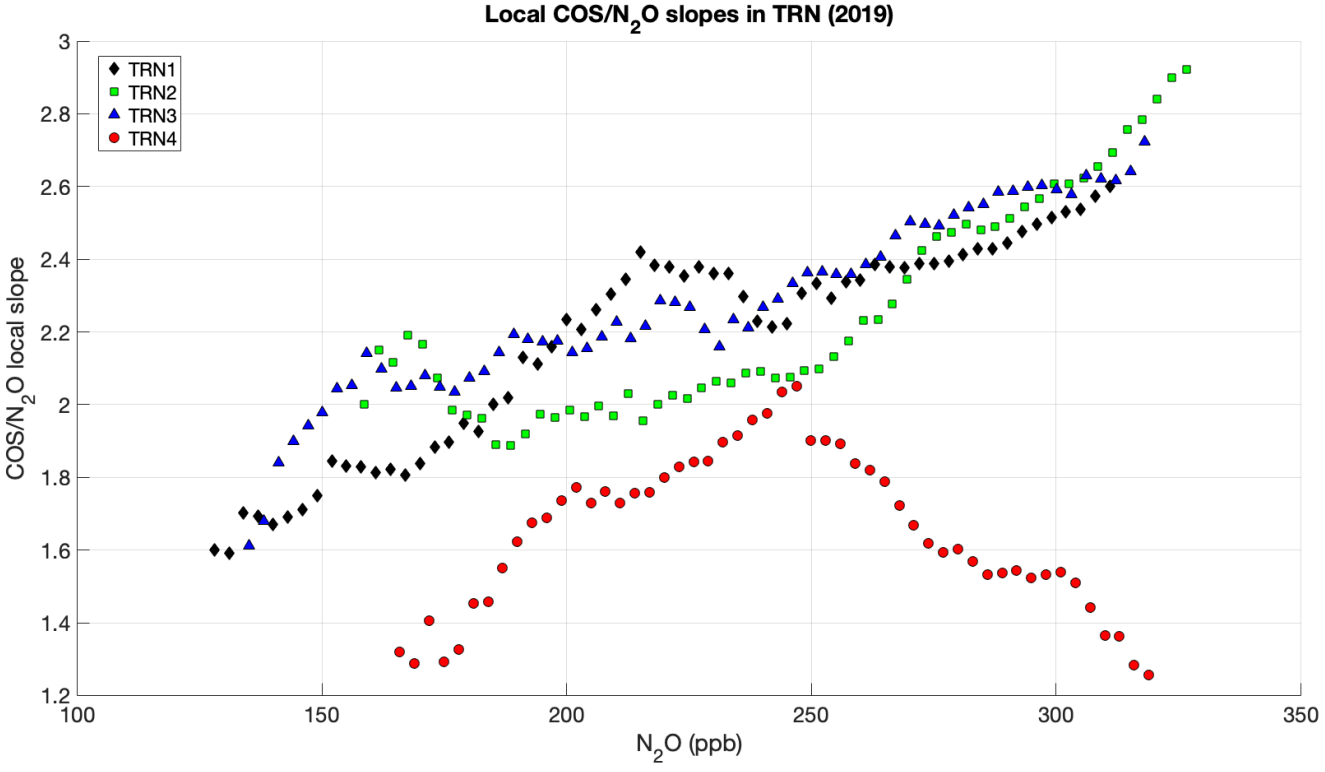

Figure 5: local COS/N_2O slopes from profiles obtained during the TRN campaign, 2019.

https://doi.org/10.5194/egusphere-2026-2799
Preprint. Discussion started: 1 June 2026

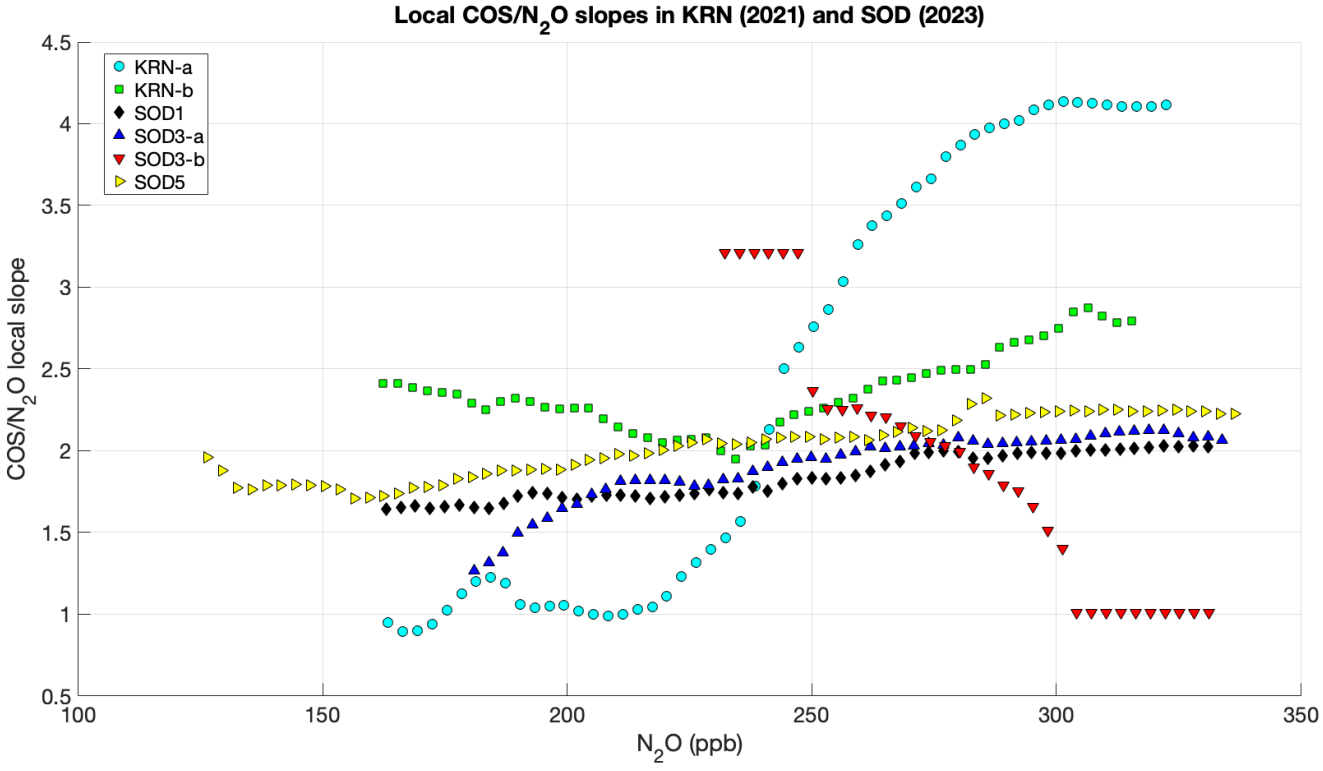

Figure 6: local COS/N_2O slopes from profiles obtained during the KRN campaign, 2021, and the SOD campaign, 2023.

https://doi.org/10.5194/egusphere-2026-2799
Preprint. Discussion started: 1 June 2026

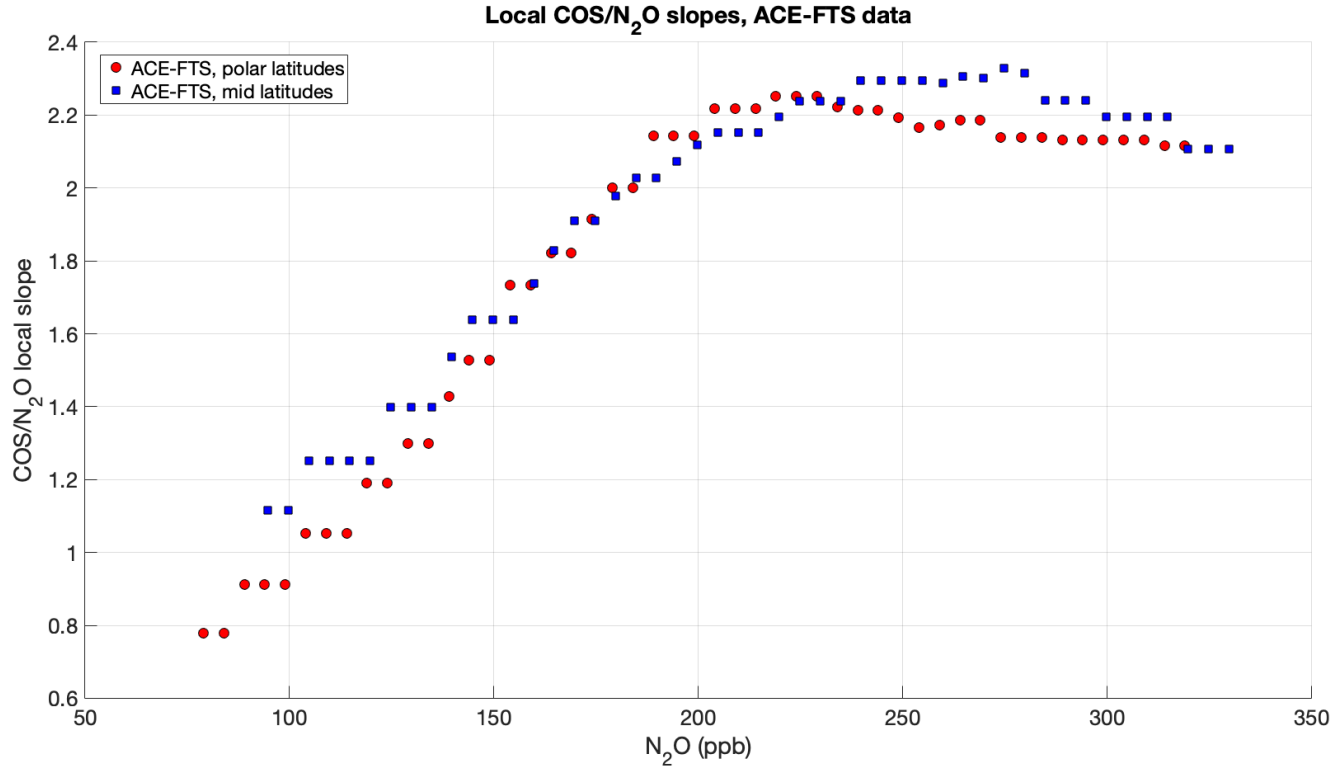

Figure 7: local COS/N_2O slopes from profiles obtained averaging the ACE-FTS datasets at polar and mid latitudes.

https://doi.org/10.5194/egusphere-2026-2799
Preprint. Discussion started: 1 June 2026

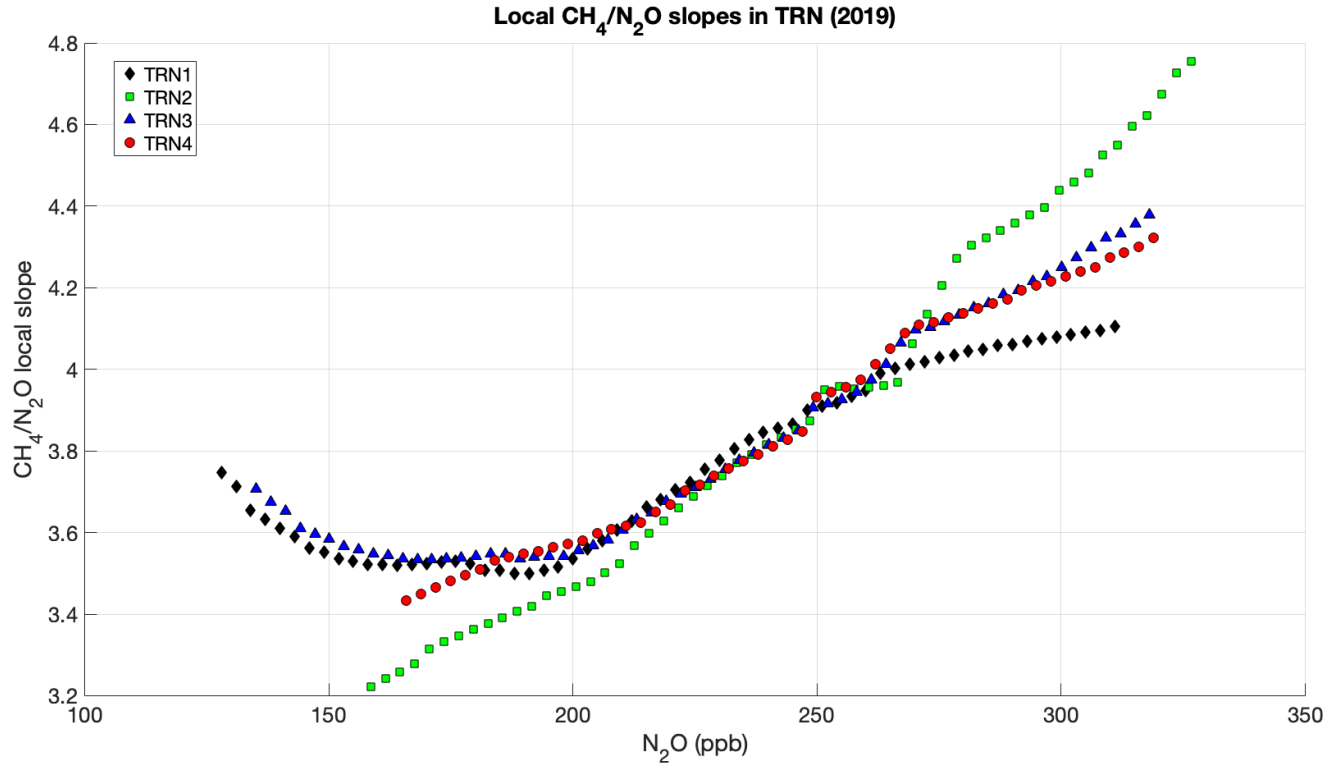

Figure 8: local CH_4/N_2O slopes from profiles obtained during the TRN campaign, 2019.

https://doi.org/10.5194/egusphere-2026-2799
Preprint. Discussion started: 1 June 2026

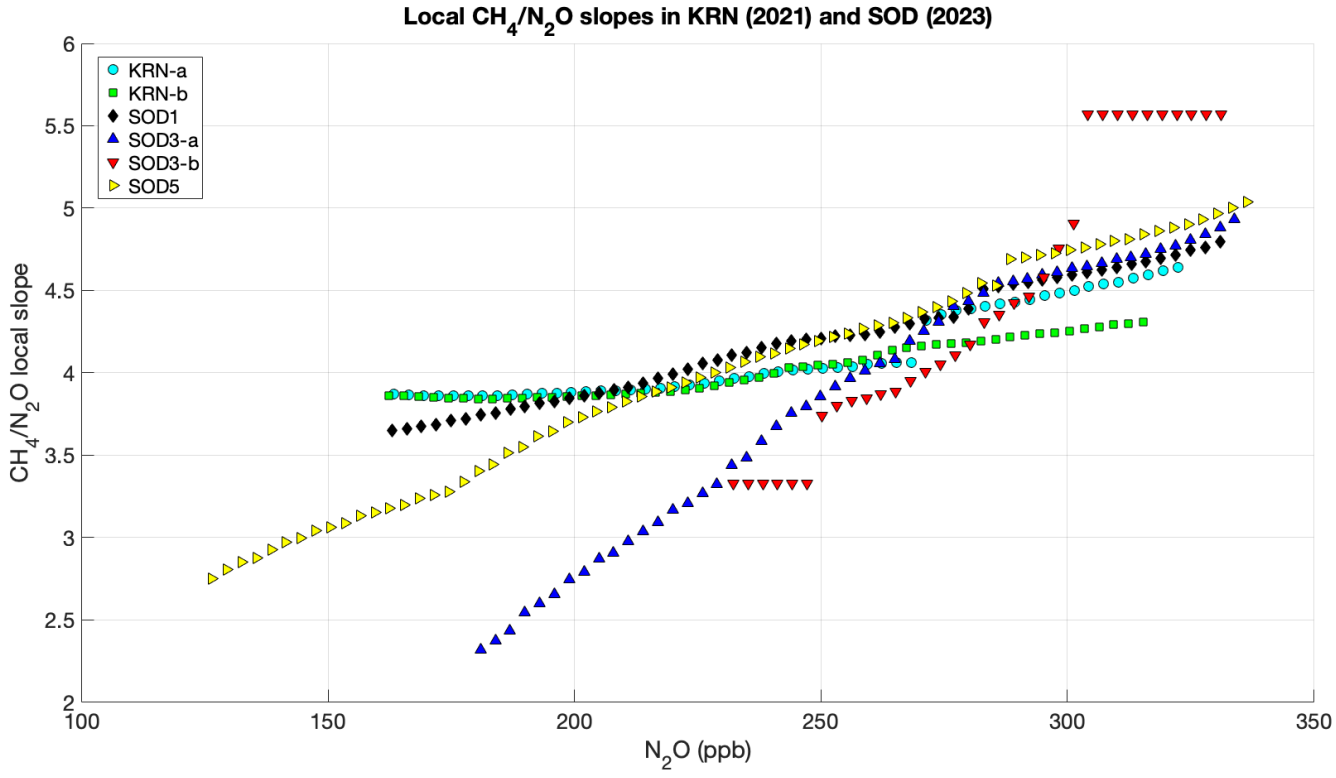

Figure 9: local CH_4/N_2O slopes from profiles obtained during the KRN campaign, 2021, and the SOD campaign, 2023.

https://doi.org/10.5194/egusphere-2026-2799
Preprint. Discussion started: 1 June 2026

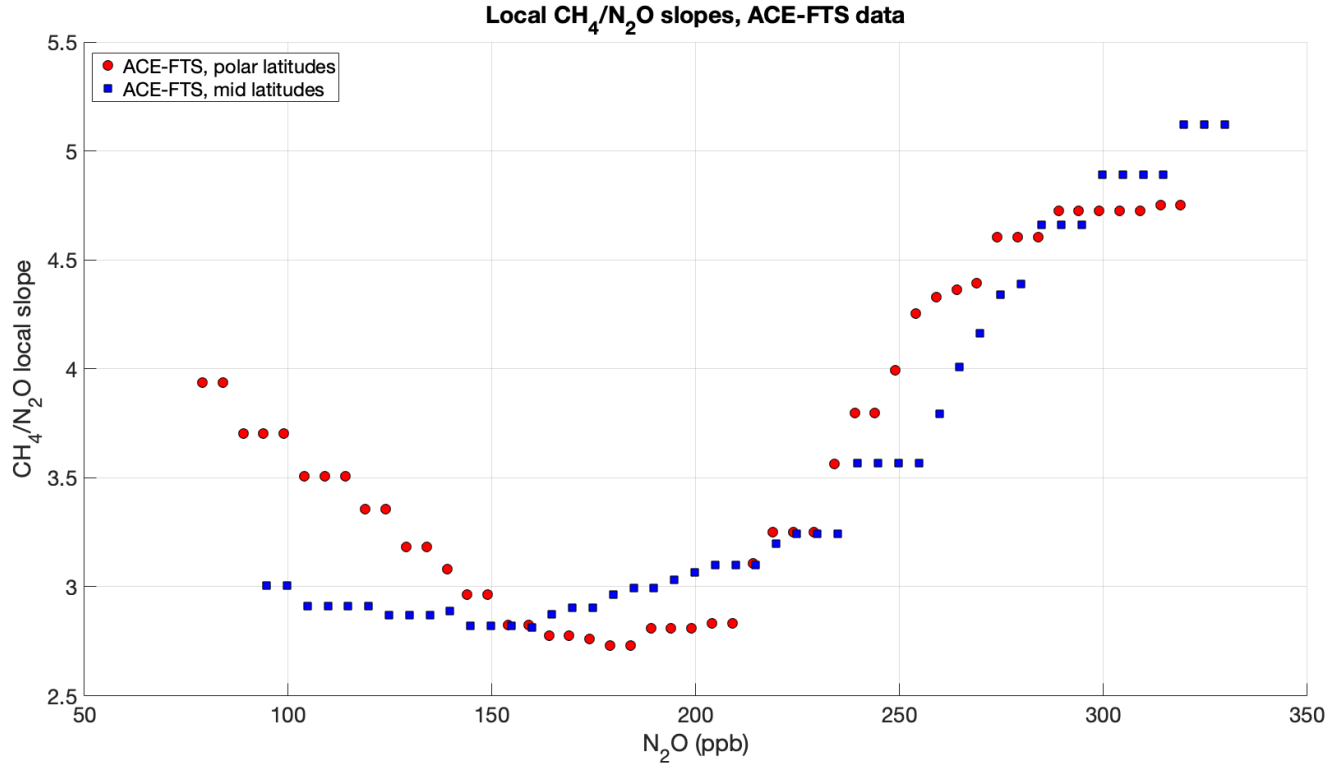

Figure 10: local CH_4/N_2O slopes from profiles obtained averaging the ACE-FTS datasets at polar and mid latitudes.

2.5.3 Data deficiency and flagging of outliers

Figures 5–8 show the local slopes against N_2O for both COS and CH_4 obtained from data collected during sampling campaigns. Consistently to what was observed with the Plumb and Ko (1992) method, KRN-a, KRN-b and SOD3-b show clearly different behaviours when compared to the other profiles. As discussed previously, the measured KRN-a profiles showed significantly lower COS mole fractions between 17–20 km altitude, approximately corresponding to the selected N_2O range. This feature is also reflected in the estimated local slopes, which were therefore considered an outlier. KRN-b slopes are affected by missing data in the lower stratospheric section of the profile (roughly between 10.5–13.5 km). SOD3-b, instead, was refined due to observed contaminations–the restricted data range and the data gaps over the profile determined caused the local slopes to be significantly different from the ones of other flights, and therefore were considered not reliable. A similar issue is noticeable for the COS local slopes of TRN4. For this flight, clear signs of COS contaminations were identified between 9.3–13.9 km. These signs were not noticeable among the other measured tracers. The missing COS data determined the local linear regressions to be performed over less data points and to be biased by the highest and lowest sides of the COS profiles, determining the downwards trend for $N_2O > 250$ ppb (Figure 5). Clear deviations from the main trends are clearly noticeable for SOD3-a and SOD3-b in the CH_4/N_2O local slopes, as well.

https://doi.org/10.5194/egusphere-2026-2799
Preprint. Discussion started: 1 June 2026

3. Results

We estimated the stratospheric lifetimes of COS and CH_4, along with their respective sinks, based on the tropospheric burdens of COS, CH_4 and N_2O and the slopes derived from stratospheric COS-N_2O and CH_4-N_2O correlations.

3.1 Atmospheric burdens

Burdens represent the atmospheric mass of a specific tracer, obtained multiplying its mole fraction by the total atmospheric mass (roughly $5.15 \cdot 10^{21}$ g). However, since the application of burdens in the given lifetime formulas requires a ratio of two tracers, the total atmospheric mass factor would be cancelled out. Therefore, we report the burdens as mean atmospheric mole fractions. COS tropospheric burdens estimated following Andrews et al. (2001) (Sect. 2.4.2) decreased from 490 ± 18 ppt in 2019 to 479 ± 21 ppt in 2021 and then increased again to 487 ± 18 ppt in 2023. Although not significant, this trend differs from the constant and significant increase of N_2O (from 332.0 ± 0.7 ppb in 2019 to 336.8 ± 2.0 ppb in 2023) and CH_4 (from 1844.6 ± 9.9 ppb in 2019 to 1899.2 ± 9.9 ppb in 2023). These burdens were applied in the Plumb and Ko (1992) method. The total atmospheric global burdens of COS, N_2O and CH_4 were also estimated to be implemented in the Volk et al. (1997) method. The total COS atmospheric burden decreases from 468 ± 9 ppt in 2019 to 457 ± 9 ppt in 2023. The total atmospheric burden of N_2O increases from 322.3 ± 2.5 ppb in 2019 to 324.0 ± 3.6 ppb in 2023, while CH_4 shows an increase from 1806.6 ± 14.1 ppb in 2019 to 1845.9 ± 20.5 ppb in 2023. These trends, reasonably, resemble the general tropospheric trends but are reduced by the weighted average with the stratospheric mole fractions.

3.2 COS

3.2.1 COS-N_2O stratospheric correlations

The correlation slopes between COS and N_2O (Table 4) will be expressed as $d\sigma_{N_2O}/d\sigma_{COS}$ (ppb/ppt), as these are the values that are implemented in Eq. (2), with the N_2O mole fraction expressed in ppb and COS mole fraction in ppt. At mid latitudes, we find an average slope of 0.431 ± 0.029 (ranging between 0.405 and 0.463 ppb/ppt). At polar latitudes, the average slope is 0.470 ± 0.048. Noticeably, SOD1 has a significantly steeper slope than the other flights. The ACE-FTS averaged profiles return a slope of 0.436 ± 0.003 ppb/ppt at mid latitudes and 0.456 ± 0.004 ppb/ppt at polar latitudes, with the low uncertainties likely ascribable to the averaging over numerous singular profiles. In both AirCore and ACE-FTS profiles the slopes at polar latitudes are generally steeper than the ones at mid latitudes.

The slopes at the tropopause (Table 6) result in averages of 0.438 ± 0.046 ppb/ppt at mid latitudes and of 0.482 ± 0.031 at polar latitudes. The corresponding ACE-FTS slopes are 0.429 ± 0.008 at mid latitudes and 0.483 ± 0.007 at polar latitudes. These $d\sigma_{N_2O}/d\sigma_{COS}$ correlation slopes extrapolated at the tropopause result to be steeper at higher latitudes, similarly to what was observed with the previous methodology.

https://doi.org/10.5194/egusphere-2026-2799
Preprint. Discussion started: 1 June 2026

3.2.2 COS stratospheric lifetime and sink estimates

The stratospheric lifetime of a tracer is unique, although its estimates may result in slight differences, depending e.g. on latitude (Krysztofiak et al., 2015). Therefore, in the following paragraphs lifetime estimates from AirCore profiles and ACE-FTS averaged profiles will be reported separately for mid and polar latitudes. The stratospheric COS lifetime calculated following Plumb and Ko (1992) range between 69–90 years, with an overall average (for latitudes > 47 °N) of 76 ± 6 years, corresponding to an average stratospheric sink of 37 ± 3 GgS yr^{-1}, ranging between 31–41 GgS yr^{-1}. The average lifetime derived from mid-latitude data in 2019 is 74 ± 5 years, while the average lifetime inferred from profiles collected at polar latitudes between 2021 and 2023 is 79 ± 9 years. Although the lifetime estimates from the most recent polar campaigns seem to be slightly longer than the ones obtained previously at mid-latitude, the difference between the two is not significant. No significant difference was found between stratospheric COS lifetime calculated from ACE-FTS observations and AirCore profiles.

Following the methodology described in Volk et al. (1997), COS lifetime falls in a range of 71–83 years, averaging at 78 ± 7 years over the lifetime estimates retrieved from AirCore data, corresponding to an average sink of 35 ± 3 GgS yr^{-1} (ranging 32–39 GgS yr^{-1}). The average lifetime derived from mid-latitude profiles is 74 ± 8 years, while the lifetime estimations derived from profiles measured at polar latitudes is 79 ± 5 years. Compared to the results obtained with the method of Plumb and Ko (1992), these lifetime estimates are not significantly different. This method, too, resulted in coherent lifetime estimates between ACE-FTS and AirCore profiles. A comparison between the lifetime obtained with the two different method is presented in Figure 11. The lifetime estimates do not differ significantly between the two methods.

Table 4: results of tropospheric burdens and stratospheric linear regression between COS and N_2O (Plumb and Ko, 1992) for all AirCore samples and ACE-FTS averages. The results marked by * shall be considered outliers.

Date/period	Data origin	COS tropospheric burden (ppt)	N_2O tropospheric burden (ppb)	N_2O/COS stratospheric slope (ppb/ppt)	N_2O/COS R-squared
17/06/2019	TRN1	490 ± 18	332.0 ± 0.7	0.409 ± 0.014	0.924
18/06/2019	TRN2			0.463 ± 0.017	0.945
18/06/2019	TRN3			0.405 ± 0.012	0.949
20/06/2019	TRN4			0.448 ± 0.018	0.938
13/08/2021	KRN-a	479 ± 21	334.6 ± 1.1	0.316 ± 0.013 *	0.847
13/08/2021	KRN-b			0.423 ± 0.011	0.943
02/08/2023	SOD1	487 ± 18	336.9 ± 2.0	0.535 ± 0.007	0.982
05/08/2023	SOD3-a			0.448 ± 0.024	0.947
05/08/2023	SOD3-b			- *	-
08/08/2023	SOD5			0.475 ± 0.006	0.989

https://doi.org/10.5194/egusphere-2026-2799
Preprint. Discussion started: 1 June 2026

June to September, 2012-present	Polar (65°-69° N) average, ACE-FTS	487 ± 18	336.9 ± 2.0	0.456 ± 0.004	0.999
June to September, 2012-present	Mid-latitude (45°-49° N) average, ACE-FTS	490 ± 18	332.0 ± 0.7	0.436 ± 0.003	0.999

Table 5: calculated COS lifetime and sink for all AirCore campaigns and ACE-FTS observations following the method described by Plumb and Ko (1992). The missing results are the ones related to outliers (see Table 4 and Sect. 2.4.4).

Date	Data origin	COS tropospheric burden (TgCOS)	COS lifetime (years)	COS stratospheric sink (GgS yr^{-1})
17/06/2019	TRN1	5.29 ± 0.10	70 ± 11	40 ± 8
18/06/2019	TRN2	5.29 ± 0.10	79 ± 12	35 ± 7
18/06/2019	TRN3	5.29 ± 0.10	69 ± 10	41 ± 7
20/06/2019	TRN4	5.29 ± 0.10	77 ± 12	36 ± 7
13/08/2021	KRN-a	5.15 ± 0.12	-	-
13/08/2021	KRN-b	5.15 ± 0.12	70 ± 10	39 ± 7
02/08/2023	SOD1	5.20 ± 0.10	90 ± 12	31 ± 5
05/08/2023	SOD3-a	5.20 ± 0.10	75 ± 13	37 ± 8
05/08/2023	SOD3-b	5.20 ± 0.10	-	-
08/08/2023	SOD5	5.20 ± 0.10	80 ± 11	35 ± 6
June to September, 2012-2023	Polar (65°-69° N) average, ACE-FTS	5.20 ± 0.10	76 ± 10	36 ± 6
June to September, 2012-2023	Mid-latitude (45°-49° N) average, ACE-FTS	5.29 ± 0.10	75 ± 9	37 ± 6

Table 6: average global atmospheric burdens of COS and N_2O and COS stratospheric lifetime and sink estimates, retrieved following the Volk et al. (1997) method. The missing results are related to slopes at the tropopause that were marked as outliers (signalled by *, see Sect. 2.5.3).

Date	Data origin	N_2O/COS slope at the tropopause	COS global atmospheric average	N_2O global atmospheric average	COS lifetime (years)	COS sink (GgS yr^{-1})
17/06/2019	TRN1	0.419 ± 0.011	468 ± 9 ppt	322.3 ± 2.5 ppb	71 ± 9	38 ± 6
18/06/2019	TRN2	0.490 ± 0.025			83 ± 13	32 ± 6
18/06/2019	TRN3	0.403 ± 0.011			68 ± 9	39 ± 6
20/06/2019	TRN4	0.728 ± 0.047 *			-	-

https://doi.org/10.5194/egusphere-2026-2799
Preprint. Discussion started: 1 June 2026

13/08/2021	KRN-a	0.198 ± 0.011 *	458 ± 15 ppt	324.2 ± 2.4 ppb	-	-
13/08/2021	KRN-b	0.346 ± 0.016 *			-	-
02/08/2023	SOD1	0.498 ± 0.011	457 ± 9 ppt	324.0 ± 3.6 ppb	81 ± 11	32 ± 5
05/08/2023	SOD3-a	0.502 ± 0.024			82 ± 13	32 ± 6
05/08/2023	SOD3-b	0.276 ± 0.056 *			-	-
08/08/2023	SOD5	0.446 ± 0.010			73 ± 9	36 ± 5
June to September, 2012-2023	Polar (65°-69° N) average, ACE-FTS	0.483 ± 0.007	457 ± 9 ppt	324.0 ± 3.6 ppb	79 ± 10	33 ± 5
June to September, 2012-2023	Mid-latitude (45°-49° N) average, ACE-FTS	0.429 ± 0.008	468 ± 9 ppt	322.3 ± 2.5 ppb	72 ± 9	37 ± 5

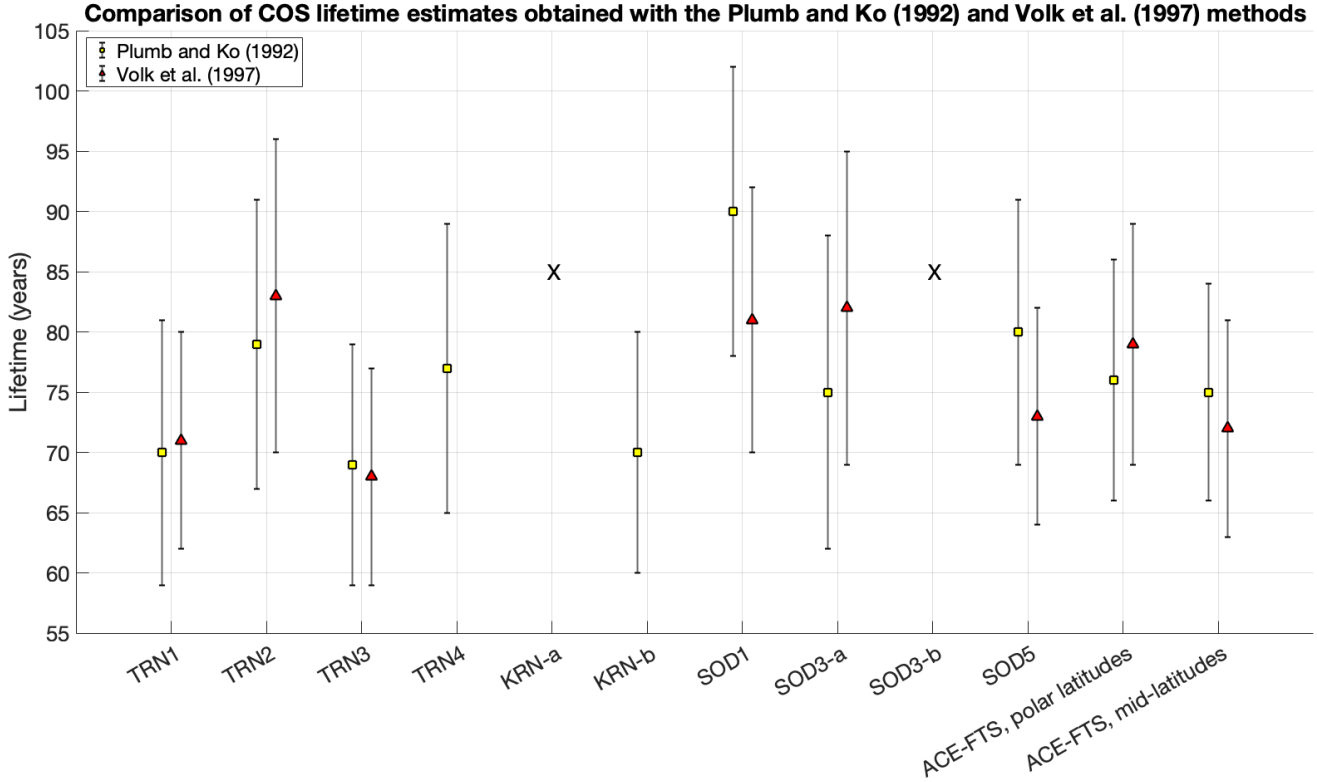

Figure 11: calculated COS lifetime for AirCore samples and ACE-FTS observations obtained following the two methodologies. Datasets for which it was not possible to apply any of the two methods reliably are signaled by an "X".

https://doi.org/10.5194/egusphere-2026-2799
Preprint. Discussion started: 1 June 2026

3.3 CH_4

3.3.1 CH_4-N_2O correlations

Similarly to COS, the slopes between CH_4 and N_2O will be expressed as $d\sigma_{N_2O}/d\sigma_{CH_4}$ in ppb/ppb (Table 7). In all cases, the R-squared values confirm a very tight relationship between the two tracers. The application of the Plumb and Ko (1992) method leads to an average slope at mid latitudes is 0.2537 ± 0.0022, while at polar latitudes is 0.2381 ± 0.0063. Interestingly, it is also possible to notice lower slopes for the SOD profiles when compared to the KRN ones. ACE-FTS averaged profiles result in a slope of 0.2217 ± 0.0053 at polar latitudes and 0.2647 ± 0.0118 at mid latitudes, in both cases slightly higher than the ones estimated from the AirCore profiles. Both slopes inferred from ACE-FTS and AirCore profiles are steeper at mid latitudes than at polar latitudes.

The application of the Volk et al. (1997) method resulted in $d\sigma_{N_2O}/d\sigma_{CH_4}$ slopes at the tropopause (Table 9) ranging between 0.2374–0.2473 at mid latitudes (with an average of 0.2416 ± 0.0043) and between 0.2361–0.2552 at polar latitudes (with an average of 0.2376 ± 0.0092). This resembles the latitudinal trends obtained with the Plumb and Ko (1992) method. However, the differences between mid and polar latitudes in this case are not significant. The slopes at the tropopause obtained from the ACE-FTS datasets are 0.2343 ± 0.0169 at mid latitudes and 0.1948 ± 0.0098 at polar latitudes, resulting again in slightly steeper slopes at mid latitudes than at polar latitudes.

3.3.2 CH_4 stratospheric lifetime and sink estimates

The stratospheric CH_4 lifetime range resulting from AirCore data with the Plumb and Ko (1992) method (Table 8) spans between 153–166 years. The lifetime estimates resulting from data collected at polar latitudes appear to be slightly shorter than the ones obtained from mid latitude observations, although the difference is not statistically significant. The consequent stratospheric sink falls within the 24–27 TgC yr^{-1}. This trend is resembled by the lifetime estimates obtained following the method of Volk et al. (1997), which yields CH_4 lifetime ranging between 149–162 years, with the shortest lifetime results obtained from datasets collected at polar latitudes. The associated stratospheric sink is 24–26 TgC yr^{-1}. A comparison between the results from both methods is presented in Figure 12. CH_4 lifetime estimates obtained with the Volk et al. (1997) method are generally shorter, although not significantly, than the ones obtained following Plumb and Ko (1992) with the biggest differences observed between the results obtained with the ACE-FTS datasets. All results will be further discussed in Sect. 4.

Table 7: tropospheric burdens (Sect 2.4.2) and stratospheric linear regression results (Sect. 2.4.3) between CH_4 and N_2O for all AirCore samples and ACE-FTS averages.

Date	Data origin	CH_4 tropospheric burden (ppb)	N_2O tropospheric burden (ppb)	N_2O/CH_4 stratospheric slope (ppb/ppb)	N_2O/CH_4 R-squared
17/06/2019	TRN1	1844.6 ± 9.9	332.0 ± 0.4	0.2516 ± 0.0006	0.999

https://doi.org/10.5194/egusphere-2026-2799
Preprint. Discussion started: 1 June 2026

18/06/2019	TRN2	1844.6 ± 9.9	332.0 ± 0.4	0.2523 ± 0.0005	0.999
18/06/2019	TRN3	1844.6 ± 9.9	332.0 ± 0.4	0.2562 ± 0.0007	0.999
20/06/2019	TRN4	1844.6 ± 9.9	332.0 ± 0.4	0.2549 ± 0.0006	0.999
13/08/2021	KRN-a	1864.3 ± 10.2	333.3 ± 0.4	0.2463 ± 0.0004	0.999
13/08/2021	KRN-b	1864.3 ± 10.2	333.3 ± 0.4	0.2432 ± 0.0004	0.999
02/08/2023	SOD1	1899.2 ± 9.9	335.9 ± 0.3	0.2352 ± 0.0002	0.999
05/08/2023	SOD3-a	1899.2 ± 9.9	335.9 ± 0.3	0.2334 ± 0.0010	0.999
05/08/2023	SOD3-b	1899.2 ± 9.9	335.9 ± 0.3	-	-
08/08/2023	SOD5	1899.2 ± 9.9	335.9 ± 0.3	0.2322 ± 0.0004	0.999
June to September, 2012-2023	Polar (65°-69° N) average, ACE-FTS	1899.2 ± 9.9	335.9 ± 0.3	0.2217 ± 0.0053	0.999
June to September, 2012-2023	Mid-latitude (45°-49° N) average, ACE-FTS	1844.6 ± 9.9	332.0 ± 0.4	0.2647 ± 0.0118	0.996

Table 8: calculated CH_4 lifetime and sink for all AirCore campaigns and ACE-FTS observations following Plumb and Ko (1992).

Date	Data origin	CH_4 tropospheric burden ($PgCH_4$)	CH_4 lifetime (years)	CH_4 stratospheric sink ($TgC\ yr^{-1}$)
17/06/2019	TRN1	5.25 ± 0.03	163 ± 15	24 ± 2
18/06/2019	TRN2	5.25 ± 0.03	163 ± 15	24 ± 2
18/06/2019	TRN3	5.25 ± 0.03	166 ± 15	24 ± 2
20/06/2019	TRN4	5.25 ± 0.03	165 ± 15	24 ± 2
13/08/2021	KRN-a	5.30 ± 0.03	161 ± 15	25 ± 3
13/08/2021	KRN-b	5.30 ± 0.03	159 ± 15	25 ± 3
02/08/2023	SOD1	5.40 ± 0.03	155 ± 15	26 ± 3
05/08/2023	SOD3-a	5.40 ± 0.03	153 ± 15	27 ± 3
05/08/2023	SOD3-b	5.40 ± 0.03	-	-
08/08/2023	SOD5	5.40 ± 0.03	153 ± 15	27 ± 3
June to September, 2012-2023	Polar (65°-69° N) average, ACE-FTS	5.40 ± 0.03	146 ± 17	28 ± 4
June to September, 2012-2023	Mid-latitude (45°-49° N) average, ACE-FTS	5.25 ± 0.03	171 ± 23	23 ± 3

https://doi.org/10.5194/egusphere-2026-2799
Preprint. Discussion started: 1 June 2026

Table 9: slopes at the tropopause, average global atmospheric burdens of CH_4 and N_2O and CH_4 stratospheric lifetime and sink estimates, retrieved following the Volk et al. (1997) method.

Date	Data origin	N_2O/CH_4 slope at the tropopause	CH_4 global atmospheric average	N_2O global atmospheric average	CH_4 lifetime (years)	CH_4 sink (TgC yr^{-1})
17/06/2019	TRN1	0.2473 ± 0.0005	1806.6 ± 14.1 ppb	322.3 ± 2.5 ppb	161 ± 15	24 ± 2
18/06/2019	TRN2	0.2394 ± 0.012			156 ± 15	25 ± 3
18/06/2019	TRN3	0.2425 ± 0.0014			158 ± 16	24 ± 3
20/06/2019	TRN4	0.2374 ± 0.0018			154 ± 16	25 ± 3
13/08/2021	KRN-a	0.2481 ± 0.0008	1825.5 ± 15.3 ppb	324.2 ± 2.4 ppb	162 ± 16	24 ± 3
13/08/2021	KRN-b	0.2401 ± 0.0008			157 ± 15	25 ± 3
02/08/2023	SOD1	0.2361 ± 0.0002	1845.9 ± 20.5 ppb	324.0 ± 3.6 ppb	156 ± 16	25 ± 3
05/08/2023	SOD3-a	-			-	-
05/08/2023	SOD3-b	-			-	-
08/08/2023	SOD5	0.2260 ± 0.0003			149 ± 15	26 ± 3
June to September, 2012-2023	Polar (65°-69° N) average, ACE-FTS	0.1948 ± 0.0098	1825.5 ± 15.3 ppb	324.0 ± 3.6 ppb	127 ± 18	31 ± 5
June to September, 2012-2023	Mid-latitude (45°-49° N) average, ACE-FTS	0.2343 ± 0.0169	1806.6 ± 14.1 ppb	322.3 ± 2.5 ppb	152 ± 25	25 ± 4

https://doi.org/10.5194/egusphere-2026-2799
Preprint. Discussion started: 1 June 2026

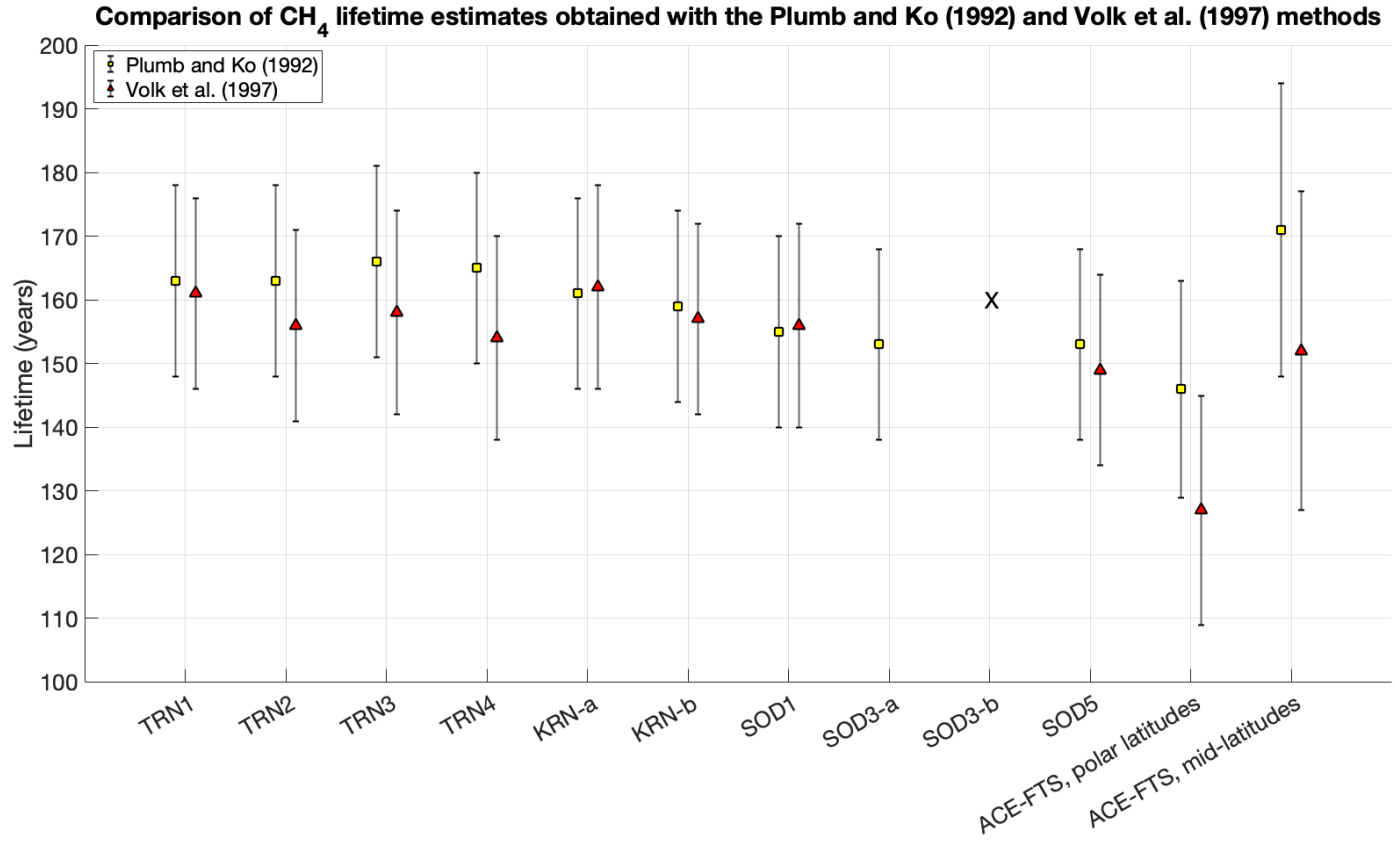

Figure 12: calculated CH_4 lifetime for AirCore samples and ACE-FTS observations obtained following the methods of Plumb and Ko (1992) and Volk et al. (1997). The missing estimates for SOD3-b are marked as an "X".

4. Discussion

In the following sections, we compare our results with previous studies regarding COS and CH_4 sources and sinks. For this study, we chose N_2O as the reference gas species with a well-constrained lifetime when applying Equations 1 and 2, following the approach of Plumb and Ko (1992) and Volk et al. (1997). The first approach aligns with most recent studies regarding COS lifetime estimations (Karu et al., 2023; Krysztofiak et al., 2015). However, the method of Plumb and Ko (1992) is derived from an idealized global mixing model, with tracers in steady state with negligible local sources or sinks. The method of Volk et al. (1997), later refined by Brown et al. (2013), is more comprehensive and formally accurate, accounting for non-diffusive fluxes across the boundary the tropics and mid-latitudes in each hemisphere. However, the equation of Plumb and Ko (1992) holds at the extratropical tropopause if the tracers are in slope equilibrium (e.g., their horizontal mixing is much faster than the vertical advection and chemical transformation) and if the difference of the extratropical correlation slopes is small between the two hemispheres (Volk et al., 1997). The tracers considered in this study are all long lived and should respect the slope equilibrium requisite. However, the higher (anthropogenic) surface emissions in the Northern Hemisphere for N_2O and CH_4

https://doi.org/10.5194/egusphere-2026-2799
Preprint. Discussion started: 1 June 2026

can influence the stratospheric air composition and disrupt the slope equilibrium, in particular in the lowermost stratosphere, which may undermine the application of the Plumb and Ko (1992) method. For example, the relatively faster increase in atmospheric CH_4 compared to N_2O can cause the tracer-tracer relationship to curve in the lowermost part of the stratospheric correlation. This may also happen due to seasonal cycles. COS long-term trends are generally less pronounced, but its photosynthesis-driven seasonal cycle is stronger in the Northern Hemisphere than in the Southern Hemisphere (Remaud et al., 2023). However, the lifetime estimates obtained in this study for both COS and CH_4 are not significantly different using each method (Figure 11 Figure 12). The tracer-tracer correlation slopes retrieved for the Plumb and Ko (1992) method were calculated over specific ranges for both COS and CH_4, to prevent biases due to the slope curvatures near the tropopause and in the higher parts of the profiles (Figure 2 and 3). Therefore, the results suggest that the local tracer-tracer correlations in the N_2O range between roughly 200 and 300 ppb may respect the conditions for the application of the Plumb and Ko (1992) method. The apparent COS lifetime ranges between 69–90 years with the Plumb and Ko (1992) method and between 71–82 years with the Volk et al. (1997) method. For CH_4, it ranges between 153–166 years following Plumb and Ko (1992), and between 149–162 years following Volk et al. (1997).

It should be noted that different studies applied different approaches to obtain lifetime estimates. Earlier studies applied the Plumb and Ko (1992) method, often using CFC-12 instead of N_2O as the reference tracer (Barkley et al., 2008; Engel and Schmidt, 1994). While this study presents data obtained by continuous sampling followed by mid-IR spectrometry analysis in a controlled laboratory environment, previous studies used different methodologies to obtain mole fractions of tracers. Engel and Schmidt (1994) collected discrete whole-air samples with a cryogenic sampler. Barkley et al. (2008) used observations obtained from solar occultation measurements from ACE-FTS in 2004-2006. Krysztofiak et al. (2015) obtained their data from the SPIRALE balloon-borne spectrometer. The results of Toon (1991) were reported by Krysztofiak et al. (2015) and they were obtained from the Jet Propulsion Laboratory (JPL) MkIV FTIR ground-based spectrometers observations. Karu et al. (2023) collected and analyzed whole-air samples in the upper troposphere/lowermost stratosphere (UT/LMS, 10-12 km).

Karu et al. (2023) introduced another point of discrepancy in the methodologies followed to estimate the stratospheric lifetime of the tracers: the altitudinal range covered by the observations. Our profiles cover altitudes roughly between 15 and 22 km, comparable with highest altitudes observed by Krysztofiak et al. (2015) and Barkley et al. (2008). While Toon (1991) and Toon et al. (2018) measured COS vertical profiles up to 40 km, Karu et al. (2023) was limited to observations between 10–12 km altitude.

As stated in Sect. 2.4.2, another noticeable methodological difference concerns the estimation of the tropospheric burden of the tracers. Since the tropospheric burden directly affects the calculation of a tracer's sink, this may be a major cause of discrepancies for such estimates, as will be discussed in the following sections.

https://doi.org/10.5194/egusphere-2026-2799
Preprint. Discussion started: 1 June 2026

4.1 COS stratospheric lifetime and sink

Figure 13 shows the results of previous studies that estimated COS stratospheric lifetime, which are also summarized in Table 10 together with the available sink estimates. These studies estimated the stratospheric sink of COS from modelling or observational efforts, with estimates ranging between 30–80 GgS yr^{-1} (Chin and Davis, 1995; Crutzen, 1976; Crutzen and Schmailzl, 1983; Ma et al., 2021; Turco et al., 1980; Weisenstein et al., 1997). Following the method of Plumb and Ko (1992) and Volk et al. (1997) our COS lifetime estimates at mid latitudes (Table 5) are not significantly different from each other and fall within a 69–83 years range. This is slightly, although not significantly, higher than previous global estimates (Barkley et al., 2008; Engel and Schmidt, 1994; Krysztofiak et al., 2015). Coherently with literature, we found slightly longer lifetime estimates from profiles collected at higher latitudes, with our results ranging between 70–90 years from data collected in the polar region (Table 5). Previous COS lifetime estimates obtained from polar latitude observations fall in a 70–76 years range (Barkley et al., 2008; Krysztofiak et al., 2015; Toon, 1991) and are not significantly different from our results (Figure 13, Table 10).

We estimate the COS stratospheric sink from the lifetime resulting from the Plumb and Ko (1992) method to be 35–41 GgS yr^{-1} from data collected at mid latitudes and 31–39 GgS yr^{-1} from data collected at polar latitudes (Table 5). Coherently, from lifetime estimates obtained with the Volk et al. (1997) method, we obtain COS sinks between 32–39 GgS yr^{-1} and 32–37 GgS yr^{-1} at mid latitudes and polar latitudes, respectively. Although the difference is not statistically significant, these values are generally smaller than most results from previous studies (30–80 GgS yr^{-1}, see Table 10). One exception is represented by Chin and Davis (1995), who estimated the stratospheric COS sink to be 30 GgS yr^{-1}. As mentioned in Sect. 2.4.2, all studies followed different approaches to define the tropospheric burden of COS. Since the sink is simply derived by the ratio between burden and lifetime, this has surely influenced the final result for each study. Additionally, a decreasing tropospheric burden is found for COS between 2015–2021, confirmed by recent observations (Belviso et al., 2022; Hannigan et al., 2022). Although the COS tropospheric burden seems to be increasing again in the more recent years, the N_2O tropospheric abundance has always been rising steadily. The opposed trends, of course, reciprocally affect the burdens' ratio in Eq. (2) leading to smaller estimates of the COS stratospheric sink for a given slope value. Furthermore, small differences can be found also in the N_2O/COS slope within each campaign (Table 4). As explained in Zanchetta et al. (2026), we speculate that daily atmospheric variability and/or interactions of COS or sampling equipment with other tracers may also cause biases in each flight, which may therefore increase the variability in the results. Another potential bias may be caused by uncertainties in altitude mapping of AirCore profiles (Karion et al., 2010; Membrive et al., 2017; Tans, 2022; Wagenhäuser et al., 2021). However, it was not possible to define the cause of these differences confidently with the available data. Overall, finding non-significant differences for neither lifetime nor sink estimates within our campaigns and with existing literature suggests no significant decreasing or increasing trends in the stratospheric sink of COS.

Table 10: calculated COS lifetime and sink estimates compared with the ones reported by previous studies. The studies marked with * inferred COS lifetime from a CFC-12/COS correlation. The studies marked with ^, similarly to this one, inferred COS lifetime

https://doi.org/10.5194/egusphere-2026-2799
Preprint. Discussion started: 1 June 2026

from a N_2O/COS correlation. The reference to Toon (1991) indicates the results from JPL MkIV interferometer previously reported by Krysztofiak et al. (2015) and is meant to acknowledge the source of the data.

Source	COS stratospheric lifetime (years)	COS stratospheric sink (GgS yr^{-1})	Remarks
This study, following Plumb and Ko (1992)	69–79 (mid latitudes) 70–90 (polar latitudes)	35–41 (mid latitudes) 31–39 (polar latitudes)	-
This study, following Volk et al. (1997)	71–83 (mid latitudes) 72–82 (polar latitudes)	32–39 (mid latitudes) 32–37 (polar latitudes)	-
Engel and Schmidt (1994) *	69 ± 28 (latitudes > 43 °N)	25–60, with a mean of 36 (global)	Arbitrary COS burden
Barkley et al. (2008) *	64 ± 21 (global) 76 ± 32 (polar)	50 ± 16 (global)	Arbitrary COS burden
Krysztofiak et al. (2015) ^	70 ± 20 (polar latitudes) 58 ± 14 (tropical latitudes) 64 ± 17 (global)	54 ± 14 (global)	Inferred COS and N_2O burdens from local tropospheric observations
Toon (1991) ^	74 ± 24 (polar)	-	Estimated by Krysztofiak et al. (2015)
Karu et al. (2023) ^	39 ± 15 (global)	55 ± 23 (global)	Inferred COS and N_2O burdens from local tropospheric observations
Crutzen (1976)	-	50 (global)	Modelled
Turco et al. (1980)	-	80 (global)	Modelled
Crutzen and Schmailzl (1983)	-	43 (global)	Modelled
Chin and Davis (1995)	-	30	Modelled

https://doi.org/10.5194/egusphere-2026-2799
Preprint. Discussion started: 1 June 2026

Weisenstein et al. (1997)	-	49	Modelled
Ma et al. (2021)	-	40	Modelled

4.1.2 Sensitivity of results to different methodologies

All the COS-N_2O slopes presented in this study are generally lower than the ones calculated by Krysztofiak et al. (2015) and Karu et al. (2023). This is most likely due to the different altitude ranges where the regressions are performed, together with day-to-day variability and different observational periods.

As illustrated in Sect. 2.4.2 and Sect. 4.1, several studies applied the Plumb and Ko (1992) method to calculate the stratospheric COS lifetime estimating tropospheric mole fractions with different methods, or choosing averaged or even arbitrary values. We tried to re-calculate these estimates, when possible, by correcting the tropospheric mole fractions with values obtained following the method of Andrews et al. (2001) presented in Sect. 2.4.2. Since the available data included tropospheric mole fractions in MLO and SMO for COS (2001-2021) and N_2O (1996-2024), it was possible to re-calculate both tropospheric burdens for the studies who investigated the stratospheric lifetime using the same tracers (Karu et al., 2023; Krysztofiak et al., 2015). On top of that, it was possible to calculate a new COS burden for Barkley et al. (2008). The parameters are listed in Table 11.

In the case of Krysztofiak et al. (2015) and Karu et al. (2023), the slopes of the tracer-tracer regressions were reported and it was possible to recalculate the stratospheric lifetime and sink of COS with new estimates of COS and N_2O tropospheric burdens. The lifetime results obtained with our method are generally shorter for Krysztofiak et al. (2015), who adopted relatively high tropospheric burdens, and generally higher for Karu et al. (2023), who instead opted for stratospheric mole fractions to infer the burdens of Equation 1. Karu et al. (2023) expressed the burdens following two different methods to define the tropopause height (following the potential vorticity and thermal definitions), but in both cases based the estimation of the burdens on stratospheric mole fractions. When it comes to sinks estimations, the differences become less marked. This is due to the nature of the calculation, which requires to divide again by the COS burden, reducing the bias related to this parameter. For Barkley et al. (2008) the estimation of the COS burden between 2006 and 2008 (the period of their campaign) is so close to the value they chose arbitrarily that no significant difference was found.

In all cases, the newly calculated lifetime and sink estimates are not significantly different from the original ones. However, the region where the regressions are performed and the estimated tropospheric burdens are critical to infer the lifetime of a tracer following the Plumb and Ko (1992) method. Overall, no clear trend in COS lifetime was observed over time nor using the original estimates of previous studies, nor with the recalculations obtained following our methodology.

https://doi.org/10.5194/egusphere-2026-2799
Preprint. Discussion started: 1 June 2026

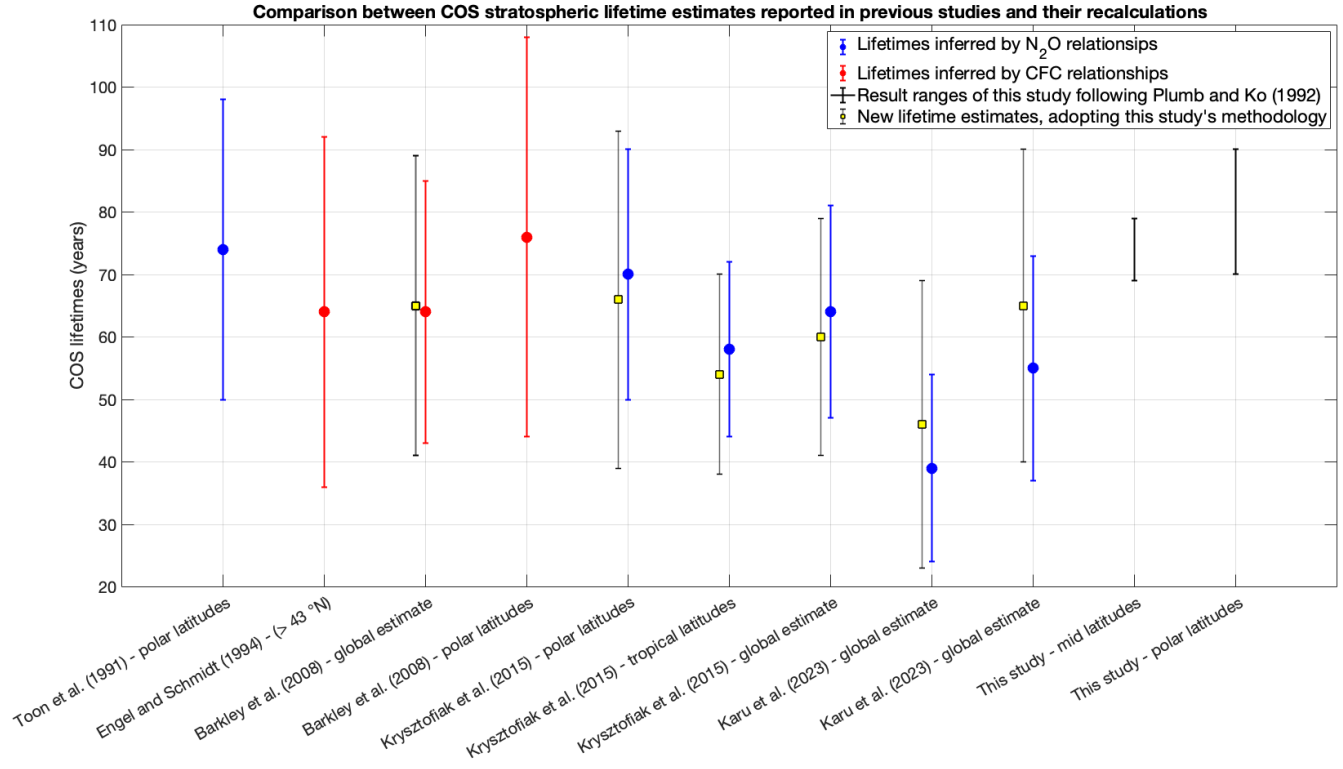

Figure 13: comparison between COS lifetime estimates of previous studies with their recalculations with new tropospheric burdens obtained following the methods of this study (based on Andrews et al., 2001), in chronological order. The ranges reported for this study correspond to the Plumb and Ko (1992) method, which was also adopted in the studies presented in this figure.

Table 11: effects of different estimations of tropospheric burdens on the final lifetime and sink estimations.

Source	Parameters used in the source study	COS lifetime in the source study (years)	COS sink in the source study (GgS yr^{-1})	Parameters following the methods of this study	COS lifetime according to the new parameters (years)	COS sink according to the new parameters (GgS yr^{-1})
SPIRALE, Krysztofiak et al. (2015)	σ_{COS} = 550 ± 40 ppt	70 ± 20 (polar latitudes) 58 ± 14 (tropical latitudes) 64 ± 17 (global)	54 ± 14 (global)	σ_{COS} = 509 ± 23 ppt	66 ± 27 (polar latitudes) 54 ± 16 (tropical latitudes) 60 ± 19 (global)	44 ± 20 (polar latitudes) 54 ± 18 (tropical latitudes) 48 ± 22 (global)
	σ_{N_2O} = 328 ± 8 ppb			σ_{N_2O} = 321 ± 1 ppb		
	T_{N_2O} = 117 ± 20 years			T_{N_2O} = 116 ± 9 years		

https://doi.org/10.5194/egusphere-2026-2799
Preprint. Discussion started: 1 June 2026

Karu et al. (2023)	σ_{COS} = 415 ± 32 ppt σ_{N_2O} = 324.0 ± 0.2 ppb T_{N_2O} = 116 ± 9 years	39 ± 15 (global, limited to 12 km), potential vorticity tropopause	55 ± 23 (global)	σ_{COS} = 502 ± 23 ppt σ_{N_2O} = 330 ± 2 ppb T_{N_2O} = 116 ± 9 years	46 ± 23 (global, limited to 12 km)	62 ± 34 (global)
	σ_{COS} = 416 ± 35 ppt σ_{N_2O} = 323.7 ± 0.2 ppb T_{N_2O} = 116 ± 9 years	55 ± 18 (global, limited to 12 km), thermal tropopause	/	σ_{COS} = 502 ± 23 ppt σ_{N_2O} = 330 ± 2 ppb T_{N_2O} = 116 ± 9 years	65 ± 25 (global, limited to 12 km)	44 ± 19 (global)
Barkley et al. (2008)	σ_{COS} = 500 ± 20% ppt	64 ± 21 (global)	34–66 (global)	σ_{COS} = 508 ± 23 ppt	65 ± 24 (global)	34–66 (global)

https://doi.org/10.5194/egusphere-2026-2799
Preprint. Discussion started: 1 June 2026

4.2 CH_4 stratospheric lifetime and sink

CH_4 stratospheric lifetime and sink were calculated following the same methodology that was followed for COS. The resulting CH_4 stratospheric lifetime estimates range between 163–166 years when inferred from mid latitude observations, and between 153–161 years from polar latitude observations (Table 8) with the Plumb and Ko (1992) method. Following the method of Volk et al. (1997), the estimates range between 154–161 years (mid latitude observations) and 149–162 (polar latitude observations) (Table 9). A generally decreasing trend is observed for CH_4 lifetime estimates from mid to polar latitudes as well as over time. However, similarly to COS, these trends are not statistically significant. Although generally higher when calculated from data collected at polar latitudes and generally lower for mid latitudes observations, CH_4 lifetime estimates from AirCore profiles do not differ significantly from their respective ACE-FTS values. These latter estimates are associated with larger uncertainties with the Volk et al. (1997) method due to larger uncertainties regarding the extrapolated slope at the tropopause for these datasets. This is due to the lower number of datapoints over which the linear regressions are performed, which affects in particular the bootstrapped values at the tropopause retrieved following Volk et al. (1997). Nevertheless, the stratospheric lifetime estimates obtained from AirCore profiles agree well with the modelled 152 and 159.6 years global estimate presented in SPARC (2013) Report No. 6 and the 159 ± 35 years inferred by Brown et al. (2013) from ACE-FTS remote sensing observations during the Northern Hemisphere Summer.

The stratospheric sink estimated from our measurements ranges between 24–25 TgC yr^{-1} from mid latitudes data and 24–26 TgC yr^{-1} from data collected at polar latitudes (Table 8, Table 9). These results are lower than earlier estimates of 34 TgC yr^{-1} (Hein et al., 1997) and 30 TgC yr^{-1} (Lelieveld et al., 1998), but fall within the more recent stratospheric loss range of 9–28 TgC yr^{-1} (Saunois et al., 2020).

Overall, within the methods applied on this study, we believe that COS and CH_4 lifetime and sink calculations share the same sources of uncertainty. Concerning CH_4, the increasing burden (Sect. 2.4.2, Sect. 2.5.2) is most likely the reason behind the slightly decreasing (although not significant) trend in stratospheric lifetime assessments. In fact, the CH_4 burden increase is relatively faster than the N_2O increase. Some small flight-to-flight variability can be observed in the N_2O/CH_4 linear regression slopes, with the slopes at polar latitudes being generally lower than the ones at mid latitudes with both methods (Table 7, Table 9). The reason behind this variability remains overall unclear. As previously speculated for COS, we believe this could be due to atmospheric transport features. Nevertheless, the resulting lifetime and sink estimates are statistically consistent with each other as well as with ACE-FTS estimates, and fall well within the ranges reported in the existing literature.

5. Conclusions

This study derived the mean stratospheric lifetime and sink of COS and CH_4 from continuous AirCore vertical profiles analyzed with a QCLS, using two methods based on the relationship of the two species with N_2O in the lower stratosphere. Stratospheric tracer-tracer correlation was found among flights, including within the same campaign. This variability may

https://doi.org/10.5194/egusphere-2026-2799
Preprint. Discussion started: 1 June 2026

reflect day-to-day changes in stratospheric transport and/or uncertainties associated with sampling and measurement, but the available information does not allow its origin to be fully understood.

Using the method of Plumb and Ko (1992), COS stratospheric lifetime was estimated at 69–79 years at mid latitudes and 70–90 years at polar latitudes, corresponding to sinks of 35–41 GgS yr^{-1} and 31–39 GgCOS yr^{-1}, respectively. Following the method of Volk et al. (1997), we find consistent results, with COS lifetime estimates of 71–83 years at mid latitudes and 72-82 years at polar latitudes, corresponding to sinks of 32–39 GgS yr^{-1} and 32-37 GgS yr^{-1}, respectively. Although these lifetime estimates are generally at the upper end of the range reported in the literature, they are not significantly different from previous values.

For CH_4, the method of Plumb and Ko (1992) yielded stratospheric lifetime ranges between 163–166 years at mid latitudes and 153–161 years at polar latitudes, while the method of Volk et al. (1997) gave lifetime estimates of 154–161 years (mid latitudes) and 149–162 (polar latitudes), respectively. Considering both methods, these ranges correspond to sink estimates of 24–25 TgC yr^{-1} and 24–26 TgC yr^{-1}.

All estimates are consistent with spatially and temporally averaged estimates based on ACE-FTS data, and with literature estimates. Overall, our results show that AirCore measurements can provide robust observational constraints on the stratospheric lifetime and sink of COS and CH_4, provide an additional tool for investigating long-term stratospheric trends, and help refine their representation in atmospheric chemistry and transport models. The results presented in this study suggest that no significant trends in stratospheric removal emerged in recent years for COS and CH_4, regardless of the observed trends for their tropospheric abundances. However, given the reported discrepancies in the methods adopted by previous studies, we advocate for a more standardized methodology for estimating the slopes and tropospheric burdens used to derive the stratospheric lifetime and sink of a tracer with these techniques.

Data availability

The data used in this work are available from https://doi.org/10.5281/zenodo.15749915 (Zanchetta et al., 2025)

Author contribution

HC conceived the concept, RK, MR, AE, HC, AZ and SvH collected the data, AZ, SvH and HC analyzed the data, MK and AE refined the employed methodologies, AZ, SvH, and HC wrote the manuscript with contribution from all authors.

Competing interests

At least one of the (co-)authors is a member of the editorial board of Atmospheric Chemistry and Physics.

Acknowledgements

https://doi.org/10.5194/egusphere-2026-2799
Preprint. Discussion started: 1 June 2026

We are grateful for the support during the preparation of the campaigns by Bert Kers, Marcel de Vries and Marc Bleeker at the Center of Isotope Research. We are grateful to Stephen Montzka (NOAA GML) for the meaningful discussion and feedback on the methods adopted in this study and for providing NOAA's datasets. We would also like to thank the colleagues who collaborated during the campaigns, especially Maria Elena Popa, Johannes Laube, Sophie Baartman and Johannes Degen.

Financial support

This research was supported by the ERC advanced funding scheme (AdG 2016 project no. 742798, project abbreviation COS-OCS), and by the Ruisdael Observatory infrastructure cofinanced by the Dutch Research Council (NWO, Grant No. 184.034.015), ICOS Netherlands and the ESA project FRM4GHG. This work was also supported by the Natural Science Foundation of China (42475115).

https://doi.org/10.5194/egusphere-2026-2799
Preprint. Discussion started: 1 June 2026

References

Andrews, A. E., Boering, K. A., Daube, B. C., Wofsy, S. C., Hintsa, E. J., Weinstock, E. M., and Bui, T. P.: Empirical age spectra for the lower tropical stratosphere from in situ observations of CO_2 : Implications for stratospheric transport, J. Geophys. Res. Atmospheres, 104, 26581–26595, https://doi.org/10.1029/1999JD900150, 1999.

Andrews, A. E., Boering, K. A., Daube, B. C., Wofsy, S. C., Loewenstein, M., Jost, H., Podolske, J. R., Webster, C. R., Herman, R. L., Scott, D. C., Flesch, G. J., Moyer, E. J., Elkins, J. W., Dutton, G. S., Hurst, D. F., Moore, F. L., Ray, E. A., Romashkin, P. A., and Strahan, S. E.: Mean ages of stratospheric air derived from in situ observations of CO_2 , CH_4 , and N_2O, J. Geophys. Res. Atmospheres, 106, 32295–32314, https://doi.org/10.1029/2001JD000465, 2001.

Barkley, M. P., Palmer, P. I., Boone, C. D., Bernath, P. F., and Suntharalingam, P.: Global distributions of carbonyl sulfide in the upper troposphere and stratosphere, Geophys. Res. Lett., 35, L14810, https://doi.org/10.1029/2008GL034270, 2008.

Belviso, S., Remaud, M., Abadie, C., Maignan, F., Ramonet, M., and Peylin, P.: Ongoing Decline in the Atmospheric COS Seasonal Cycle Amplitude over Western Europe: Implications for Surface Fluxes, Atmosphere, 13, 812, https://doi.org/10.3390/atmos13050812, 2022.

Bernath, P. F.: Atmospheric Chemistry Experiment (ACE): Mission overview, Geophys. Res. Lett., 32, L15S01, https://doi.org/10.1029/2005GL022386, 2005.

Boering, K. A., Wofsy, S. C., Daube, B. C., Schneider, H. R., Loewenstein, M., Podolske, J. R., and Conway, T. J.: Stratospheric Mean Ages and Transport Rates from Observations of Carbon Dioxide and Nitrous Oxide, Science, 274, 1340–1343, https://doi.org/10.1126/science.274.5291.1340, 1996.

Boone, C. D., Bernath, P. F., and Lecours, M.: Version 5 retrievals for ACE-FTS and ACE-imagers, J. Quant. Spectrosc. Radiat. Transf., 310, 108749, https://doi.org/10.1016/j.jqsrt.2023.108749, 2023.

Brown, A. T., Volk, C. M., Schoeberl, M. R., Boone, C. D., and Bernath, P. F.: Stratospheric lifetimes of CFC-12, CCl_4, CH_4, CH_3Cl and N_2O from measurements made by the Atmospheric Chemistry Experiment-Fourier Transform Spectrometer (ACE-FTS), Atmospheric Chem. Phys., 13, 6921–6950, https://doi.org/10.5194/acp-13-6921-2013, 2013.

Brühl, C., Lelieveld, J., Crutzen, P. J., and Tost, H.: The role of carbonyl sulphide as a source of stratospheric sulphate aerosol and its impact on climate, Atmospheric Chem. Phys., 12, 1239–1253, https://doi.org/10.5194/acp-12-1239-2012, 2012.

Chin, M. and Davis, D. D.: A reanalysis of carbonyl sulfide as a source of stratospheric background sulfur aerosol, J. Geophys. Res. Atmospheres, 100, 8993–9005, https://doi.org/10.1029/95JD00275, 1995.

Cho, A., Kooijmans, L. M. J., Driever, S. M., Wassenaar, M., Koren, G., Baartman, S. L., Mossink, L., and Krol, M. C.: Leaf chamber experiments on sunflowers indicate a temperature-dependent compensation point of carbonyl sulfide, Open Res. Eur., 5, 223, https://doi.org/10.12688/openreseurope.20235.2, 2025.

Crutzen, P. J.: The possible importance of CSO for the sulfate layer of the stratosphere, Geophys. Res. Lett., 3, 73–76, https://doi.org/10.1029/GL003i002p00073, 1976.

Crutzen, P. J. and Schmailzl, U.: Chemical budgets of the stratosphere, Planet. Space Sci., 31, 1009–1032, https://doi.org/10.1016/0032-0633(83)90092-2, 1983.

Engel, A. and Schmidt, U.: Vertical profile measurements of carbonylsulfide in the stratosphere, Geophys. Res. Lett., 21, 2219–2222, https://doi.org/10.1029/94GL01461, 1994.

https://doi.org/10.5194/egusphere-2026-2799
Preprint. Discussion started: 1 June 2026

Glatthor, N., Höpfner, M., Leyser, A., Stiller, G. P., Von Clarmann, T., Grabowski, U., Kellmann, S., Linden, A., Sinnhuber, B.-M., Krysztofiak, G., and Walker, K. A.: Global carbonyl sulfide (OCS) measured by MIPAS/Envisat during 2002–2012, Atmospheric Chem. Phys., 17, 2631–2652, https://doi.org/10.5194/acp-17-2631-2017, 2017.

Gurganus, C., Rollins, A., Waxman, E., Pan, L. L., Smith, W. P., Ueyama, R., Feng, W., Chipperfield, M. P., Atlas, E. L., Schwarz, J. P., DeLone, S., and Thornberry, T.: Highlighting the Impact of Anthropogenic OCS Emissions on the Stratospheric Sulfur Budget With In Situ Observations, J. Geophys. Res. Atmospheres, 130, e2024JD042588, https://doi.org/10.1029/2024JD042588, 2025.

Hannigan, J. W., Ortega, I., Shams, S. B., Blumenstock, T., Campbell, J. E., Conway, S., Flood, V., Garcia, O., Griffith, D., Grutter, M., Hase, F., Jeseck, P., Jones, N., Mahieu, E., Makarova, M., De Mazière, M., Morino, I., Murata, I., Nagahama, T., Nakijima, H., Notholt, J., Palm, M., Poberovskii, A., Rettinger, M., Robinson, J., Röhling, A. N., Schneider, M., Servais, C., Smale, D., Stremme, W., Strong, K., Sussmann, R., Te, Y., Vigouroux, C., and Wizenberg, T.: Global Atmospheric OCS Trend Analysis From 22 NDACC Stations, J. Geophys. Res. Atmospheres, 127, e2021JD035764, https://doi.org/10.1029/2021JD035764, 2022.

Hein, R., Crutzen, P. J., and Heimann, M.: An inverse modeling approach to investigate the global atmospheric methane cycle, Glob. Biogeochem. Cycles, 11, 43–76, https://doi.org/10.1029/96GB03043, 1997.

Karion, A., Sweeney, C., Tans, P., and Newberger, T.: AirCore: An Innovative Atmospheric Sampling System, J. Atmospheric Ocean. Technol., 27, 1839–1853, https://doi.org/10.1175/2010JTECHA1448.1, 2010.

Karu, E., Li, M., Ernle, L., Brenninkmeijer, C. A. M., Lelieveld, J., and Williams, J.: Carbonyl Sulfide (OCS) in the Upper Troposphere/Lowermost Stratosphere (UT/LMS) Region: Estimates of Lifetimes and Fluxes, Geophys. Res. Lett., 50, e2023GL105826, https://doi.org/10.1029/2023GL105826, 2023.

Kaushik, A., Miller, J., Montzka, S., Hu, L., Sweeney, C., McKain, K., Baker, I., Haynes, K., Denning, S., and Andrews, A.: Alaskan regional-scale measurements show late season ecosystem carbonyl sulfide uptake decoupled from gross photosynthesis, Environ. Res. Lett., 21, 054002, https://doi.org/10.1088/1748-9326/ae4045, 2026.

Kloss, C., Von Hobe, M., Höpfner, M., Walker, K. A., Riese, M., Ungermann, J., Hassler, B., Kremser, S., and Bodeker, G. E.: Sampling bias adjustment for sparsely sampled satellite measurements applied to ACE-FTS carbonyl sulfide observations, Atmospheric Meas. Tech., 12, 2129–2138, https://doi.org/10.5194/amt-12-2129-2019, 2019.

Krysztofiak, G., Té, Y. V., Catoire, V., Berthet, G., Toon, G. C., Jégou, F., Jeseck, P., and Robert, C.: Carbonyl Sulphide (OCS) Variability with Latitude in the Atmosphere, Atmosphere-Ocean, 53, 89–101, https://doi.org/10.1080/07055900.2013.876609, 2015.

Laube, J. C., Keil, A., Bönisch, H., Engel, A., Röckmann, T., Volk, C. M., and Sturges, W. T.: Observation-based assessment of stratospheric fractional release, lifetimes, and ozone depletion potentials of ten important source gases, Atmospheric Chem. Phys., 13, 2779–2791, https://doi.org/10.5194/acp-13-2779-2013, 2013.

Leedham Elvidge, E. C., Bönisch, H., Brenninkmeijer, C. A. M., Engel, A., Fraser, P. J., Gallacher, E., Langenfelds, R., Mühle, J., Oram, D. E., Ray, E. A., Ridley, A. R., Röckmann, T., Sturges, W. T., Weiss, R. F., and Laube, J. C.: Evaluation of stratospheric age of air from CF_4, C_2F_6, C_3F_8, CHF_3, HFC-125, HFC-227ea and SF_6; implications for the calculations of halocarbon lifetimes, fractional release factors and ozone depletion potentials, Atmospheric Chem. Phys., 18, 3369–3385, https://doi.org/10.5194/acp-18-3369-2018, 2018.

Lelieveld, J., Crutzen, P. J., and Dentener, F. J.: Changing concentration, lifetime and climate forcing of atmospheric methane, Tellus B Chem. Phys. Meteorol., 50, 128, https://doi.org/10.3402/tellusb.v50i2.16030, 1998.

https://doi.org/10.5194/egusphere-2026-2799
Preprint. Discussion started: 1 June 2026

Leung, F. T., Colussi, A. J., Hoffmann, M. R., and Toon, G. C.: Isotopic fractionation of carbonyl sulfide in the atmosphere: Implications for the source of background stratospheric sulfate aerosol, Geophys. Res. Lett., 29, https://doi.org/10.1029/2001GL013955, 2002.

Ma, J., Kooijmans, L. M. J., Cho, A., Montzka, S. A., Glatthor, N., Worden, J. R., Kuai, L., Atlas, E. L., and Krol, M. C.: Inverse modelling of carbonyl sulfide: implementation, evaluation and implications for the global budget, Atmospheric Chem. Phys., 21, 3507–3529, https://doi.org/10.5194/acp-21-3507-2021, 2021.

Membrive, O., Crevoisier, C., Sweeney, C., Danis, F., Hertzog, A., Engel, A., Bönisch, H., and Picon, L.: AirCore-HR: a high-resolution column sampling to enhance the vertical description of CH_4 and CO_2, Atmospheric Meas. Tech., 10, 2163–2181, https://doi.org/10.5194/amt-10-2163-2017, 2017.

Montzka, S. A., Calvert, P., Hall, B. D., Elkins, J. W., Conway, T. J., Tans, P. P., and Sweeney, C.: On the global distribution, seasonality, and budget of atmospheric carbonyl sulfide (COS) and some similarities to CO_2, J. Geophys. Res., 112, D09302, https://doi.org/10.1029/2006JD007665, 2007.

NOAA: Scientific assessment of Ozone depletion: 2002. Persuant to Article 6 of the Montreal Protocol on substances that deplete the ozone layer, World Meteorological Organization, Geneva, 500 pp., 2003.

Plumb, R. A. and Ko, M. K. W.: Interrelationships between mixing ratios of long-lived stratospheric constituents, J. Geophys. Res. Atmospheres, 97, 10145–10156, https://doi.org/10.1029/92JD00450, 1992.

Prather, M. J., Hsu, J., DeLuca, N. M., Jackman, C. H., Oman, L. D., Douglass, A. R., Fleming, E. L., Strahan, S. E., Steenrod, S. D., Søvde, O. A., Isaksen, I. S. A., Froidevaux, L., and Funke, B.: Measuring and modeling the lifetime of nitrous oxide including its variability, J. Geophys. Res. Atmospheres, 120, 5693–5705, https://doi.org/10.1002/2015JD023267, 2015.

Prather, M. J., Froidevaux, L., and Livesey, N. J.: Observed changes in stratospheric circulation: decreasing lifetime of N_2O, 2005–2021, Atmospheric Chem. Phys., 23, 843–849, https://doi.org/10.5194/acp-23-843-2023, 2023.

Remaud, M., Ma, J., Krol, M., Abadie, C., Cartwright, M. P., Patra, P., Niwa, Y., Rodenbeck, C., Belviso, S., Kooijmans, L., Lennartz, S., Maignan, F., Chevallier, F., Chipperfield, M. P., Pope, R. J., Harrison, J. J., Vimont, I., Wilson, C., and Peylin, P.: Intercomparison of Atmospheric Carbonyl Sulfide (TransCom-COS; Part One): Evaluating the Impact of Transport and Emissions on Tropospheric Variability Using Ground-Based and Aircraft Data, J. Geophys. Res. Atmospheres, 128, e2022JD037817, https://doi.org/10.1029/2022JD037817, 2023.

Saunois, M., Stavert, A. R., Poulter, B., Bousquet, P., Canadell, J. G., Jackson, R. B., Raymond, P. A., Dlugokencky, E. J., Houweling, S., Patra, P. K., Ciais, P., Arora, V. K., Bastviken, D., Bergamaschi, P., Blake, D. R., Brailsford, G., Bruhwiler, L., Carlson, K. M., Carrol, M., Castaldi, S., Chandra, N., Crevoisier, C., Crill, P. M., Covey, K., Curry, C. L., Etiope, G., Frankenberg, C., Gedney, N., Hegglin, M. I., Höglund-Isaksson, L., Hugelius, G., Ishizawa, M., Ito, A., Janssens-Maenhout, G., Jensen, K. M., Joos, F., Kleinen, T., Krummel, P. B., Langenfelds, R. L., Laruelle, G. G., Liu, L., Machida, T., Maksyutov, S., McDonald, K. C., McNorton, J., Miller, P. A., Melton, J. R., Morino, I., Müller, J., Murguia-Flores, F., Naik, V., Niwa, Y., Noce, S., O'Doherty, S., Parker, R. J., Peng, C., Peng, S., Peters, G. P., Prigent, C., Prinn, R., Ramonet, M., Regnier, P., Riley, W. J., Rosentreter, J. A., Segers, A., Simpson, I. J., Shi, H., Smith, S. J., Steele, L. P., Thornton, B. F., Tian, H., Tohjima, Y., Tubiello, F. N., Tsuruta, A., Viovy, N., Voulgarakis, A., Weber, T. S., van Weele, M., van der Werf, G. R., Weiss, R. F., Worthy, D., Wunch, D., Yin, Y., Yoshida, Y., Zhang, W., Zhang, Z., Zhao, Y., Zheng, B., Zhu, Q., Zhu, Q., and Zhuang, Q.: The Global Methane Budget 2000–2017, Earth Syst. Sci. Data, 12, 1561–1623, https://doi.org/10.5194/essd-12-1561-2020, 2020.

https://doi.org/10.5194/egusphere-2026-2799
Preprint. Discussion started: 1 June 2026

Serio, C., Montzka, S. A., Masiello, G., and Carbone, V.: Trend and Multi-Frequency Analysis Through Empirical Mode Decomposition: An Application to a 20-Year Record of Atmospheric Carbonyl Sulfide Measurements, J. Geophys. Res. Atmospheres, 128, e2022JD038207, https://doi.org/10.1029/2022JD038207, 2023.

SPARC: SPARC Report on the Lifetimes of Stratospheric Ozone-Deleting Substances, Their Replacements, and Related Species., 2013.

Spielmann, F. M., Kitz, F., Roach, T., Kranner, I., Hammerle, A., and Wohlfahrt, G.: Effects of drought on carbonyl sulfide exchange in four plant species, Plant Stress, 15, 100735, https://doi.org/10.1016/j.stress.2024.100735, 2025.

Stimler, K., Nelson, D., and Yakir, D.: High precision measurements of atmospheric concentrations and plant exchange rates of carbonyl sulfide using mid-IR quantum cascade laser, Glob. Change Biol., https://doi.org/10.1111/j.1365-2486.2009.02088.x, 2009.

Stimler, K., Montzka, S. A., Berry, J. A., Rudich, Y., and Yakir, D.: Relationships between carbonyl sulfide (COS) and CO_2 during leaf gas exchange, New Phytol., 186, 869–878, https://doi.org/10.1111/j.1469-8137.2010.03218.x, 2010.

Stimler, K., Berry, J. A., and Yakir, D.: Effects of Carbonyl Sulfide and Carbonic Anhydrase on Stomatal Conductance, Plant Physiol., 158, 524–530, https://doi.org/10.1104/pp.111.185926, 2012.

Tans, P.: Fill dynamics and sample mixing in the AirCore, Atmospheric Meas. Tech., 15, 1903–1916, https://doi.org/10.5194/amt-15-1903-2022, 2022.

Tong, X., Van Heuven, S., Scheeren, B., Kers, B., Hutjes, R., and Chen, H.: Aircraft-Based AirCore Sampling for Estimates of N_2O and CH_4 Emissions, Environ. Sci. Technol., 57, 15571–15579, https://doi.org/10.1021/acs.est.3c04932, 2023.

Toon, G. C.: The JPL MkIV interferometer, Opt. Photonics News, 2, 19, https://doi.org/10.1364/OPN.2.10.000019, 1991.

Toon, G. C., Blavier, J.-F. L., and Sung, K.: Atmospheric carbonyl sulfide (OCS) measured remotely by FTIR solar absorption spectrometry, Atmospheric Chem. Phys., 18, 1923–1944, https://doi.org/10.5194/acp-18-1923-2018, 2018.

Turco, R. P., Whitten, R. C., Toon, O. B., Pollack, J. B., and Hamill, P.: OCS, stratospheric aerosols and climate, Nature, 283, 283–285, https://doi.org/10.1038/283283a0, 1980.

Velazco, V. A., Toon, G. C., Blavier, J.-F. L., Kleinböhl, A., Manney, G. L., Daffer, W. H., Bernath, P. F., Walker, K. A., and Boone, C.: Validation of the Atmospheric Chemistry Experiment by noncoincident MkIV balloon profiles, J. Geophys. Res., 116, D06306, https://doi.org/10.1029/2010JD014928, 2011.

Vernier, J.-P., Thomason, L. W., Pommereau, J.-P., Bourassa, A., Pelon, J., Garnier, A., Hauchecorne, A., Blanot, L., Trepte, C., Degenstein, D., and Vargas, F.: Major influence of tropical volcanic eruptions on the stratospheric aerosol layer during the last decade, Geophys. Res. Lett., 38, n/a-n/a, https://doi.org/10.1029/2011GL047563, 2011.

Vinković, K., Andersen, T., De Vries, M., Kers, B., Van Heuven, S., Peters, W., Hensen, A., Van Den Bulk, P., and Chen, H.: Evaluating the use of an Unmanned Aerial Vehicle (UAV)-based active AirCore system to quantify methane emissions from dairy cows, Sci. Total Environ., 831, 154898, https://doi.org/10.1016/j.scitotenv.2022.154898, 2022.

Volk, C. M., Elkins, J. W., Fahey, D. W., Dutton, G. S., Gilligan, J. M., Loewenstein, M., Podolske, J. R., Chan, K. R., and Gunson, M. R.: Evaluation of source gas lifetimes from stratospheric observations, J. Geophys. Res. Atmospheres, 102, 25543–25564, https://doi.org/10.1029/97JD02215, 1997.

https://doi.org/10.5194/egusphere-2026-2799
Preprint. Discussion started: 1 June 2026

Wagenhäuser, T., Engel, A., and Sitals, R.: Testing the altitude attribution and vertical resolution of AirCore measurements with a new spiking method, Atmospheric Meas. Tech., 14, 3923–3934, https://doi.org/10.5194/amt-14-3923-2021, 2021.

Weisenstein, D. K., Yue, G. K., Ko, M. K. W., Sze, N., Rodriguez, J. M., and Scott, C. J.: A two-dimensional model of sulfur species and aerosols, J. Geophys. Res. Atmospheres, 102, 13019–13035, https://doi.org/10.1029/97JD00901, 1997.

Whelan, M. E., Lennartz, S. T., Gimeno, T. E., Wehr, R., Wohlfahrt, G., Wang, Y., Kooijmans, L. M. J., Hilton, T. W., Belviso, S., Peylin, P., Commane, R., Sun, W., Chen, H., Kuai, L., Mammarella, I., Maseyk, K., Berkelhammer, M., Li, K.-F., Yakir, D., Zumkehr, A., Katayama, Y., Ogée, J., Spielmann, F. M., Kitz, F., Rastogi, B., Kesselmeier, J., Marshall, J., Erkkilä, K.-M., Wingate, L., Meredith, L. K., He, W., Bunk, R., Launois, T., Vesala, T., Schmidt, J. A., Fichot, C. G., Seibt, U., Saleska, S., Saltzman, E. S., Montzka, S. A., Berry, J. A., and Campbell, J. E.: Reviews and syntheses: Carbonyl sulfide as a multi-scale tracer for carbon and water cycles, Biogeosciences, 15, 3625–3657, https://doi.org/10.5194/bg-15-3625-2018, 2018.

Wilson, J. C., Lee, S.-H., Reeves, J. M., Brock, C. A., Jonsson, H. H., Lafleur, B. G., Loewenstein, M., Podolske, J., Atlas, E., Boering, K., Toon, G., Fahey, D., Bui, T. P., Diskin, G., and Moore, F.: Steady-state aerosol distributions in the extra-tropical, lower stratosphere and the processes that maintain them, Atmospheric Chem. Phys., 8, 6617–6626, https://doi.org/10.5194/acp-8-6617-2008, 2008.

World Meteorological Organization (WMO): Meteorology – A three-dimensional science: Second session of the Commission for Aerology, 1957.

Zanchetta, A., Van Heuven, S., Hooghiem, J., Kivi, R., Laemmel, T., Ramonet, M., Leuenberger, M., Nyfeler, P., Baartman, S. L., Krol, M., and Chen, H.: Balloon-borne stratospheric vertical profiling of carbonyl sulfide and evaluation of ozone scrubbing materials, Atmospheric Meas. Tech., 19, 1465–1486, https://doi.org/10.5194/amt-19-1465-2026, 2026.